Published in final edited form as:
Brain Res. 2010 July 16; 1344: 104–123. doi:10.1016/j.brainres.2010.05.003.

Immunohistochemical Localization of AMPA Type Glutamate Receptor Subunits in the Striatum of Rhesus Monkey

Yun-Ping Deng, **Evan Shelby**, and **Anton J. Reiner**
Department of Anatomy & Neurobiology, University of Tennessee Health Science Center, Memphis, TN 38163

Abstract

Corticostriatal and thalamostriatal projections utilize glutamate as their neurotransmitter. Their influence on striatum is mediated, in part, by ionotropic AMPA-type glutamate receptors, which are heteromers composed of GluR1-4 subunits. While the cellular localization of AMPA-type subunits in the basal ganglia has been well characterized in rodents, the cellular localization of AMPA subunits in primate basal ganglia is not. We thus carried out immunohistochemical studies of GluR1-4 distribution in rhesus monkey basal ganglia in conjunction with characterization of each major neuron type. In striatum, about 65% of striatal neurons immunolabeled for GluR1, 75%-79% immunolabeled for GluR2 or GluR2/3, and only 2.5% possessed GluR4. All neurons the large size of cholinergic interneurons (mean diameter 26.1μm) were moderately labeled for GluR1, while all neurons in the size range of parvalbuminergic interneurons (mean diameter 13.8μm) were intensely rich in GluR1. Additionally, somewhat more than half of neurons in the size range of projection neurons (mean diameter 11.6μm) immunolabeled for GluR1, and about one third of these were very rich in GluR1. About half of neurons the size of cholinergic interneurons were immunolabeled for GluR2, and the remainder of the neurons that were immunolabeled for GluR2 coincided with projection neurons in size and shape (GluR2 diameter=10.7μm), indicating that the vast majority of striatal projection neurons possess immunodectible GluR2. Similar results were observed with GluR2/3 immunolabeling. Half of the neurons the size of cholinergic interneurons immunolabeled for GluR4 and seemingly all neurons in the size range of parvalbuminergic interneurons possessed GluR4. These results indicate that AMPA receptor subunit combinations for striatal projection neurons in rhesus monkey are similar to those for the corresponding neuron types in rodents, and thus their AMPA responses to glutamate likely to be similar to those demonstrated in rodents.

Keywords

Basal Ganglia; glutamate receptors; glutamate; monkey

1. Introduction

The basal ganglia receives a prominent glutamatergic input from the cerebral cortex and from the thalamus (Somogyi et al., 1981; Gerfen, 1992). Corticostriatal and thalamostriatal terminals are known to make excitatory asymmetric synaptic contacts with the spines and

Address Correspondence to: Dr. Yun-Ping Deng, Department of Anatomy & Neurobiology, University of Tennessee Health Science Center, 855 Monroe Avenue, Memphis, TN 38163, Phone: 901-448-8256, Fax: 901-448-7193, ydeng@uthsc.edu.

dendrites of striatal projection neurons (Wilson, 1995; Reiner et al, 2003; Lei et al., 2004; Smith et al., 2001, 2004), as well as with the dendrites of parvalbuminergic and calretinergic striatal interneurons (Bennett and Bolam, 1993a, 1994; Kawaguchi, 1993; Kawaguchi et al., 1995). Consistent with these glutamatergic inputs, neurons in the striatum are rich in glutamate receptors (Chen et al., 1996; Götz et al., 1997; Deng et al., 2007). The response of basal ganglia neurons to excitatory input from cerebral cortex and thalamus has been shown to be mediated by three types of ionotropic glutamate receptors, the L-amino-3-hydroxy-5-methyl-4-isoxazolepropionic acid (AMPA) type, the N-methyl-D-aspartate (NMDA) type, and the kainic acid (KA) type (Götz et al., 1997; Calabresi et al., 1998; Stefani et al., 1998). AMPA-type, NMDA-type, and KA-type receptors are multimeric transmembrane proteins consisting of combinations of any of several type-specific subunits that form ligand-gated ion channels permeable to cations such as Ca^{2+} and Na+ (Mayer and Armstrong, 2004).

AMPA receptors are the main glutamate receptor type that mediates the fast excitatory response of neurons to glutamatergic input, and they are formed from combinations of the glutamate receptor subunits GluR1–4 (Keinanen et al., 1990; Seeburg, 1993; Hollman and Heinemann, 1994). The subunit composition of AMPA-type glutamate receptors influences their divalent ion permeability, rectification, sensitivity to polyamines, and kinetics (Seeburg, 1993; Hollman and Heinemann, 1994; Jonas and Burnashev, 1995). Immunohistochemical and *in situ* hybridization studies in rodents have demonstrated that most basal ganglia neurons possess AMPA receptor subunits, with neuron type-specific differences in subunit composition (Tallaksen-Greene and Albin, 1994; Chen et al., 1996; Paquet and Smith, 1996; Kwok et al., 1997; Deng et al., 2007). For example, in rats medium-sized spiny GABAergic striatal projection neurons are enriched in GluR1, GluR2 and/or GluR3, whereas parvalbuminergic and cholinergic aspiny GABAergic striatal interneurons are enriched in GluR1 and/or GluR4 (Tallaksen-Greene and Albin, 1994; Bernard et al., 1996; Chen et al., 1996, 1998; Paquet and Smith, 1996; Kwok et al., 1997; Stefani et al., 1998; Deng et al., 2007). The differential expression of AMPA-type receptor subunits in projection neurons and interneurons may explain differences among these neuron types in their AMPA-mediated responses to glutamate or cortical excitation (Götz et al., 1997; Calabresi et al., 1998; Stefani et al., 1998; Vorobjev et al., 2000).

AMPA receptors have been identified in monkey (Martin et al., 1993a) and human basal ganglia (Meng et al., 1997; Tomiyama et al., 1997) by *in situ* hybridization histochemistry and immunohistochemistry, but detailed information on the types of neurons possessing the different AMPA subunits in monkey basal ganglia is not available. We thus used immunohistochemistry to characterize the size, shape and abundance of perikarya possessing GluR1-4 AMPA subunits in the striatum of rhesus monkey. Data on the size, shape and abundance of the various striatal neuron types allowed us to use AMPA subunit localization to clarify the AMPA subunits on specific basal ganglia neuron types.

2. Results

2.1 Projection neurons and interneurons in caudate and putamen in rhesus monkey

With increasing age, the autofluorescent pigment lipofuscin accumulates in neurons. The presence of lipofuscin granules complicates the use of fluorescence microscopy in the central nervous system because of its broad excitation and emission spectra, which overlaps with those of most commonly used fluorophores (Brizzee et al., 1974; Bardon, 1980). Though some chemical reagents may reduce the autofluorescence in rodent brain sections, they incompletely remove lipofuscin autofluorescence in primate brain sections (Schnell et al., 1999). Since this was the case for the present tissue, we could not carry out double immunofluorescence labeling. Since our goal was to relate AMPA subunit localization to the defined types of basal ganglia neurons in monkey, we therefore carried out

immunohistochemical single-label studies in rhesus monkey, using: 1) immunolabeling of markers of the various striatal neuron types to define the size and frequency of each in caudate and putamen; and 2) antibodies against the main AMPA subunits to define the size and frequency of the neurons possessing these subunits in caudate and putamen. In this way, we were able to shed light on the AMPA subunit composition of the major types of striatal projection neurons and interneurons in rhesus monkey. Calbindin D28K (CALB) was used to identify striatal projection neurons of the matrix compartment, and characterize the size, shape and overall frequency of striatal projection neurons (Cote et al., 1991). Choline acetyltransferase (ChAT), calretinin (CALR), parvalbumin (PARV), somatostatin (SS) were used as markers to identify cholinergic, calretinergic, parvalbuminergic, and somatostatinergic striatal neurons (Kawaguchi et al., 1995; Deng et al., 2007). Note that somatostatinergic striatal neurons also commonly contain neuropeptide Y and nitric oxide synthase. NeuN was used as a marker to detect all striatal neuron perikarya (Mullen et al., 1992). Immunolabeling of striatal perikarya for NeuN was intense and unequivocal, with labeling evident in both the nucleus and the perikaryal cytoplasm (Fig. 1). Counts of NeuN+ neurons was used to determine total striatal neuron abundance per unit area, and used to calculate the frequency of projection neurons and interneuron types in caudate and putamen as a percent of all striatal neurons.

Calbindin and Projection Neurons—Numerous medium-sized CALB-immunolabeled perikarya were observed throughout the caudate and putamen. In both structures, CALB immunolabeling was evident in perikarya and in the neuropil of the striatal matrix compartment (Fig. 2). Small patches poor in CALB, representing the striosomal compartment, were scattered within the matrix, especially in the caudate. The CALB-negative patches of caudate were easily detected, and thus our counts of CALB+ neurons avoided striosomes and represent the matrix CALB+ neuronal frequency. Within the matrix compartment, we found that 95.1% of all caudate perikarya (i.e. of all NeuN+ neurons) contained CALB. The vast majority of these are likely to represent projection neurons, given their size and shape (Table 1 and 2). Although a subset of CALB+ striatal neurons in rodents and primates has been shown to contain SS and possess SS+ interneuron size and aspiny dendrites, in prior studies these were found to make up less than 1% of CALB+ neurons (Bennett and Bolam, 1993b;Kubota et al., 1993;Prensa et al., 1998). Our results thus suggest that about 94% of caudate matrix neurons in rhesus are CALB+ projection neurons, and likely represent all caudate matrix projection neurons (Table 3). Since interneuron frequency appears similar in the striosomal and matrix compartments (Kawaguchi et al., 1995), it seems likely that about 94% of neurons throughout caudate and putamen are projection neurons.

In dorsolateral putamen, CALB+ neurons were fewer and commonly more lightly labeled than in caudate or the remainder of the putamen, as noted previously by others for primates and rodents (Gerfen et al., 1985; Cote et al., 1991; Francois et al., 1994). Additionally, CALB-negative patches were observed in putamen, but often difficult to distinguish from fiber bundles. We therefore randomly counted CALB+ neuron throughout putamen, and some counted fields included the dorsolateral putamen and others possible striosomal territory. Accordingly, we found that CALB+ neurons were scarcer overall in putamen than in caudate matrix - 82.8% of all putamen perikarya contained CALB. Based on the frequency of CALB+ matrix projection neurons in caudate, it seems likely that about 11% of all putamen neurons are CALB-negative striatal projection neurons of the striosomal and dorsolateral putamen compartments. Across both striatal compartments, the size of CALB+ neurons ranged from 7–16μm and the average perikaryal diameter was 11.4μm, with less than 1% greater than 15μm in diameter (Tables 1 and 2, Fig. 4). The perikarya tended to be round, oval or triangular in shape.

Cholinergic Neurons—ChAT immunolabeling was found only in large striatal perikarya, and their cell size ranged from 17μm to 42μm (mean size 26.6μm), with 98% of them ≥19μm (Table 1; Fig. 4). Labeling was found in round, triangular, or polygonal perikarya with thin primary and secondary dendritic branches usually extending over 50 μm from the cell body (Fig. 2). They were uniformly distributed in the caudate and putamen, and made up 1% of the striatal neuron population (Table 2).

Parvalbuminergic Neurons—PARV-immunolabeled neurons possessed medium-sized to large perikarya with a size range from 10μm to 25μm (mean size 14.3 μm) (Table 1), which was clearly larger than that for the CALB+ medium-sized projection neurons, and 95% of them were 10–18μm (Fig. 4). The mean size of PARV+ neurons in caudate was slightly larger than that of those in putamen (Table 1). The perikarya of the PARV+ interneurons were typically elongate and less commonly round, with fine dendritic arbors, and they made up 1.7% of the total striatal perikaryal population (Fig. 2). The frequency of PARV+ perikarya in the caudate was only about half that in the putamen (Table 2).

Calretinergic Neurons—Both large and medium-sized neurons in striatum were immunolabeled for CALR (Figs. 3 and 4). Together they made up about 9.1% of striatal neurons in caudate and 4.2% in putamen (Table 2). The large CALR+ neurons possessed moderately immunolabeled round or polygonal perikaryal (mean size 26.1μm), numerous aspiny dendritic branches, and constituted 0.3% of striatal neurons in both caudate and putamen (Tables 1 and 2). Prior studies have shown these to represent a subset of the cholinergic interneurons, and our data indicates that the large CALR+ neurons represent 27% and 30% of cholinergic neurons in caudate and putamen, respectively (Table 3). Intense immunolabeling was found in the medium-sized CALR+ perikarya, whose size ranged from 7–16μm (mean size 11.4μm) (Fig. 4). Their perikarya were round, or oval (Fig. 3). The medium-sized CALR+ neurons made up 8.8% and 3.9% of striatal neurons in caudate and putamen, respectively, and some possessed immunolabeled dendrites lacking obvious spines, while others possessed little or no dendritic labeling (Table 2). Medium-sized CALR+ neurons in rats make up 0.5% of striatal neurons and have been shown to be interneurons (Bennett and Bolam, 1993a;Kawaguchi et al., 1995;Figueredo-Cardenas et al., 1996b;Rymar et al., 2004). Our findings for projection neuron frequency (94%) and for cholinergic, PARV+ and SS+ interneuron frequency (which sum to 4–5%) in the rhesus striatum suggest, by contrast, that only about 1–2% of striatal neurons are medium-sized CALR+ interneurons. This leads to the conclusion that the majority of the medium-sized CALR+ neurons in caudate and putamen are projections neurons (Table 3). As addressed in the Discussion, there is prior evidence that many medium-sized CALR+ neurons in primate striatum are projection neurons.

Somatostatinergic Neurons—SS+ neurons were also medium-sized, ranging from 9–18μm in size (mean size=13μm), and scattered throughout both caudate and putamen (Table 1; Fig. 4)). SS+ perikarya were round or oval in shape, with primary dendrites occasionally seen (Fig. 3). SS+ perikarya constituted about 1.5% of all striatal neurons (Table 2).

2.2 Localization of AMPA receptor subunits in caudate and putamen in rhesus monkey

GluR1—For GluR1, immunoreactive perikarya were prominent, abundant and widespread in striatum - 65.9% of caudate neurons and 63.4% of putamen neurons contained perikaryal GluR1 (Table 2). The immunolabeled perikarya included those of numerous medium-sized neurons (8–18μm) and less frequent large neurons (19–32μm) (Table 1; Figs. 5 and 6). Distinct neuropil immunolabeling was also evident for GluR1 throughout the striatum. The GluR1 neuropil labeling was non-uniform in the caudate and putamen, with small patches of more intense neuropil immunolabeling evident. These GluR1-rich patches have been show

to represent striosomes in monkeys (Martin et al., 1993a). The most common GluR1-immunoreactive neuron type was moderately labeled, had a uniform regional distribution within striatum, and possessed medium-sized perikarya whose size range and mean matched that of striatal projection neurons (Table 1; Figs. 5). This GluR1+ neuron type made up 46.4% of all striatal neurons (Table 2), and their perikaryal size distribution matched that of projection neurons (Fig. 7A). Accordingly, these GluR1+ perikarya appear to predominantly represent striatal projection neurons. Note that the size distribution of the medium-sized moderately immunolabeled GluR1+ perikarya showed two peaks. These two peaks lined up with a CALB+ projection neuron peak at 10μm and suggested a second less evident CALB+ projection neuron peak at 12μm. These two peaks may represent the two major types of striatal projection neurons, the direct pathway substance P-containing type and the indirect pathway enkephalinergic type.

Large (≥19μm), moderately GluR1+ neuronal perikarya also were evident (25.1μm mean diameter), and they constituted 1.3% of all striatal neurons (Tables 1 and 2). Dendritic labeling was typically poor in these neurons (Figs. 5 and 6). Based on their size, shape and frequency, the large GluR1+ perikarya seem to include all cholinergic interneurons, plus the few ≥19μm striatal PARV+ neurons that represent 0.10% of all striatal neurons.

A final group of GluR1-immunolabeled striatal neurons (18.4% and 15.3% of striatal neurons in caudate and putamen, respectively) was distinguished by the fact that they were much more intensely labeled than were the moderately labeled GluR1+ perikarya (Table 2). The intensely GluR1+ neurons were slightly more abundant in caudate than putamen, and they were not concentrated in the GluR1-rich neuropil patches representing the striosomal compartment. The perikarya of these intensely GluR1-rich neurons ranged from medium (<19μm) to large (≥19μm) in size (Tables 1 and 2). The medium-sized predominated among the intensely GluR1+ perikarya and were slightly larger in mean size (12.8μm diameter) than were projection neurons as a whole (CALB+ neurons, 11.3μm), while the large intensely GluR1+ perikarya made up only 0.2% of all striatal neurons and were 22.9μm in diameter (Tables 1 and 2). Based on their rounded shape and their size frequency distribution, the medium-sized intensely GluR1+ neurons appear to mainly represent a subset of projection neurons at the large end of the projection neuron size range (Fig. 7A). Given their size and frequency, the large intensely GluR1+ perikarya are likely to include all PARV+ interneurons ≥19μm (which make up 0.1% of all striatal neurons and have a mean size of 20.9μm), and 10% of the cholinergic interneurons. The intense GluR1+ neurons, however, included a subset that possessed rounded or elongate perikarya in the size range of PARV+ interneurons, with labeling of 1–3 primary aspiny dendrites (constituting 3.1% of all striatal neurons). According to their shape and size frequency distribution that matches the PARV+ neuron size frequency distribution (Fig. 7B), the perikarya that were intensely GluR1+ and possessed labeled aspiny dendrites appear to include the medium-sized and the few large PARV+ interneurons. It is also possible that the intensely GluR1+ neurons with or without dendrites include some projection neurons, CALR+ interneurons or SS+ interneurons, since some of these fall in the size range of the medium-sized intensely GluR1+ striatal in rhesus.

GluR2—GluR2-immunolabeled perikarya were also abundant and widely distributed in striatum (Figs. 5 and 7). Labeling in perikarya for GluR2 was typically confined to the cytoplasm, with nuclei unlabeled, and no evident dendritic labeling (Fig. 8). Unlike GluR1, perikaryal immunolabeling for GluR2 among the different-sized striatal neurons was of uniform intensity. About 77% of neurons in caudate and 80% in putamen were immunolabeled for GluR2, with the vast majority of the GluR2+ neurons (98.2%) possessing perikaryal diameters ≤16μm. Since we found that all projections neuron perikarya are in this size range, and since the size frequency distribution of GluR2+

perikarya closely matches that of the CALB+ projection neurons (Fig. 7C), our data show that about 75% of striatal projection neurons possessed immunodetectible GluR2. The medium-sized GluR2+ neurons in monkey striatum may also include PARV+, SS+, and/or CALR+ interneurons, since most PARV+ neurons, all SS+ neurons, and all medium-sized CALR+ neurons fall within the 8–18μm perikaryal diameter range in which GluR2+ neurons were the most common. The results for the 17–18μm size range, in which PARV+ neurons predominate, indicate that some PARV+ interneurons do possess GluR2, since in this size range the frequency of GluR2+ perikarya largely matches the frequency of all striatal perikarya. We also found that 0.6% of GluR2+ neurons possessed perikarya with diameters ≥19 μm (Tables 1 and 2; Fig. 5). Since 1% of all striatal neurons are ChAT+ interneurons and about 0.1% are large PARV+ neurons, our results suggest that about half of cholinergic neurons in rhesus contain GluR2. The diameters of the large GluR2 perikarya was 24.2 μm, which is slightly smaller than the mean for ChAT+ interneurons, suggesting that the large GluR2+ neurons include some PARV+ neurons and/or suggesting that the GluR2+ cholinergic neurons tend toward the smaller cholinergic neurons.

GluR2/3—The GluR2/3+ perikaryal immunolabeling in caudate and putamen largely resembled that for GluR2, and overall GluR2/3+ neurons composed 75.1% of all striatal neurons (Table 1 and 2; Figs. 5 and 9). Like GluR2, labeling in perikarya for GluR2/3 was typically confined to the cytoplasm, and no evident dendritic labeling was observed (Fig. 8). Both large and medium-sized perikarya were immunolabeled for GluR2/3, with medium-sized neurons greatly predominant. The close match of the size frequency distribution of CALB+ perikarya to the size distribution of GluR2/3+ perikarya suggests that GluR2/3 immunolabeling was localized mainly to projection neurons (Fig. 7C). Large GluR2/3+ neurons made up 1.1% of all striatal neurons (Table 2), suggesting that about half of the cholinergic interneurons possess GluR2 and half GluR3, plus all large PRV+ interneurons.

GluR4—GluR4 immunolabeling was found in only a small percentage of striatal neurons (2.4%), and GluR4-immunolabeled neurons fell into two size classes: neurons with medium to moderately large perikarya (9–18μm) and neurons with large perikarya (≥19μm) (Tables 1 and 2; Fig. 5). In both types, immunolabeling intensity was moderate to intense (Fig. 9). The large GluR4-immunolabeled neurons made up 0.5% of all striatal neurons and the medium-sized made up 1.9%. Since ChAT interneurons made up 1% of all striatal neurons in monkey, our data suggest that GluR4 is expressed in about half of ChAT+ interneurons, and some of the large PARV+ interneurons. This interpretation is consistent the size frequency distribution of these immunolabeled neuron types (Fig. 7D). The medium-sized GluR4 perikarya were usually round, oval or polygonal, without evident dendritic labeling, and their mean size was greater than that of CALB+ projection neurons and comparable to that of the medium-sized PARV+ interneurons (Table 2; Fig. 4). Moreover, the shape and size frequency distribution of the medium-sized GluR4+ neurons closely matched that of the PARV+ interneurons for the entire striatum (Fig. 7D). Thus, it seems likely the vast majority of the PARV+ interneurons less than 19μm in diameter possess GluR4, although we cannot exclude the possibility that among the medium-sized GluR4+ perikarya are some belonging to large projection neurons, SS+ neurons or medium-sized CALR+ neurons.

AMPA Summary—The AMPA subunits were widely expressed in caudate and putamen of rhesus monkey. There were no obvious differences in expression between caudate and putamen for GluRs. For GluR1, intense labeling appeared to be present in PARV+ interneurons and in a subset of projection neurons at the high end of the projection neuron size range (constituting 14% of all striatal neurons), moderate labeling in about half of projection neurons, and moderate labeling in all large cholinergic interneurons (Table 4). Since some CALR+ and all SS+ interneurons are also medium-sized, we cannot exclude the

possibility that GluR1 is expressed in some of these as well. About 75% of medium-sized striatal perikarya, and 60% of large striatal perikarya immunolabeled for GluR2, suggesting GluR2 is present in the vast majority of medium-sized projection neurons, and about half of the cholinergic interneurons in rhesus monkey striatum (Table 4). It may be that projection neurons poor in GluR1 are among those rich in GluR2, and vice versa. Since some CALR+ and PARV+ neurons, and all SS+ neurons are medium-sized, we cannot exclude the possibility that GluR2 is expressed in some of these as well. Our GluR2/3 immunolabeling suggests about half of cholinergic neurons may possess GluR3. GluR4 appears to be present in about half of cholinergic neurons. While GluR4 also is likely to be present in the majority of PARV+ interneurons, since GluR4+ perikarya were not as abundant in lateral striatum as were PARV+ interneurons, it seems that not all PARV+ interneurons possess GluR4 (Table 4).

3. Discussion

Previous ISHH and immunohistochemical studies have demonstrated AMPA receptors in humans and monkeys, but only limited information has been available on the regional or cellular localization of AMPA subunits in primate striatum. The following sections consider the implications of our findings for the understanding of the regional and cellular distribution of the AMPA-type glutamate receptor subunits in primate striatum.

3.1 Implication for AMPA receptor subunit composition and function of striatal neurons

3.1.1 Striatal Projection Neurons—All striatal projection neurons in rats express GluR2 mRNA, most express GluR1 mRNA, but few express significant levels of GluR3 mRNA, and none express GluR4 (Chen et al., 1998; Stefani et al., 1998; Vorobjev et al., 2000). Immunohistochemical studies have confirmed that all projection neuron perikarya contain GluR2 protein, and shown that 50–70% of striatal projection neuron perikarya possess GluR1 (Bernard et al., 1996, 1997; Chen et al., 1996, 1998; Deng et al., 2007), but none possess GluR4 (Bernard et al., 1996, 1997; Chen et al., 1996, 1998; Kwok et al., 1997). Consistent with prominent glutamatergic inputs to striatum from the cortex and thalamus in primates (Selemon and Goldman-Rakic, 1985; Smith et al., 2004), GluR1-4 mRNAs have been reported to be present in human caudate and putamen as well (Tomiyama et al., 1997), and immunolabeling studies have reported GluR1 and GluR2/3 immunoreactivity in human striatal neurons (Meng et al., 1997). We found that about 65% and 80% of striatal neurons in rhesus monkey immunolabeled for GluR1 and GluR2, respectively. Given our estimate that about 94% of neurons in rhesus striatum are projection neurons, and given the size frequency distribution and shape of the GluR1+ and GluR2+ neurons in monkey striatum, our data indicate that about 75% of striatal projection neurons possess immunodetectible GluR2, but only 60% possess immunodetectible GluR1. In rats as well, striatal projection neurons possess GluR2 more commonly than GluR1 (Deng et al., 2007). Our GluR1 and GluR2 frequencies in rhesus monkey suggest that many striatal projection neurons in monkeys must possess both GluR1 and GluR2, while others may be enriched in one but not the other. Few if any projection neurons in rhesus appear to contain GluR4 in their perikarya, since we found that fewer than 3% of striatal neurons labeled for GluR4 and the size frequency distribution of these indicates that PARV+ interneurons and cholinergic interneurons account for the vast majority of these.

In the present study, we further found that GluR1 immunolabeling was intense in about 15%-18% of medium-sized striatal neurons. GluR1 enrichment in medium-sized PARV+ is likely to account for that subset of GluR1-intense perikarya also possessing dendritic labeling, but based on the low frequency of PARV+ interneurons (1.7%) it is evident that the majority of the GluR1-rich striatal neurons in rhesus must be projection neurons, and make

up about 14% of projection neurons. The identity of this striatal projection neuron type could not be determined here, but they do appear to be among the larger projection neurons. In our prior study, we found that the perikarya of striato-GPe neurons tend to be richer in GluR1 than striato-GPi and striatonigral neurons (Deng et al., 2007). Based on these data (Deng et al., 2007), it is possible that the GluR1+ projection neurons of monkey striatum are enkephalinergic neurons. On the other hand, studies in mice, cats and ferrets suggest that enkephalinergic striatal neurons may have slightly narrower perikarya than do substance P-containing striatal neurons (Izzo et al., 1987; Gertler et al., 2008). Although we observed an enrichment of the striosomal neuropil in the caudate for GluR1, the intensely GluR1+ perikarya were not confined to striosomes and thus did not disproportionately represent striosomal neurons. In any event, given that the GluR1 subunit is unique among AMPA subunits in its multiple phosphorylation sites that affect AMPA receptor conductance (Santos et al., 2009), knowing which striatal projection neurons are enriched in GluR1 would be important for knowing which are most likely to show learning- or drug-mediated changes in synaptic AMPA receptor conductance that are phosphorylation-dependent (Snyder et al., 2000).

3.1.2 Striatal interneurons

Parvalbuminergic Interneurons: Studies in rats indicate that parvalbuminergic striatal interneurons receive their primary excitatory input from cerebral cortex, mainly as asymmetric axodendritic synaptic contacts (Kita et al., 1990, Kita, 1993), with the axons of PARV+ interneurons forming symmetrical synaptic contacts on somata and dendrites of projection neurons (Kita et al., 1990; Lapper et al., 1992). The observation in rats that PARV+ interneurons fire phasically at high frequency in rapid response to cortical stimulation (Kawaguchi, 1993; Kita, 1993) suggests that they should have relatively high expression of AMPA receptor subunits. Previous studies in rats reported that all PARV+ interneurons, in fact, are rich in GluR1 and GluR4, and the majority possess GluR2 as well (Martin et al., 1993b; Tallaksen-Greene and Albin, 1994; Chen et al., 1996; Bernard et al., 1997; Kwok et al., 1997; Deng et al., 2007). In the present study, we found that PARV+ neurons were more abundant in putamen than in caudate in rhesus monkey, which is different from previous reports on squirrel monkeys that reported more PARV+ neurons in caudate than in putamen (Wu and Parent, 2000). Our result for rhesus is, however, consistent with that in rats, in which PARV+ neurons are more abundant laterally than medially in striatum (Kita, 1993; Kawaguchi et al., 1995), which may indicate an important role for feedforward inhibition from PARV+ interneurons to striatal projection neurons in somatomotor striatum in primates and rodents both (Koos and Tepper, 1999). We found that PARV+ perikarya in rhesus striatum ranged in size from 10 to 25μm (Kawaguchi et al., 1995, Parent et al., 1996), with diameters typically slightly larger than those of projection neurons. The prominent responsiveness of PARV+ interneurons to cortical activation in monkeys (Parthasarathy and Graybiel, 1997) suggests that they should also be rich in AMPA receptors. As discussed above, we observed a population of intensely GluR1+ perikarya with aspiny dendrites in rhesus that were very similar to PARV+ interneurons in shape, size, frequency and regional distribution. We also found GluR4 in neurons in shape, size, frequency and regional distribution of PARV+ interneurons. It is thus likely that PARV + striatal interneurons in monkey are rich in GluR1, and GluR4 as well. We also found evidence from size range comparisons that some possess GluR2.

Cholinergic Interneurons: Large aspiny interneurons that label by ISHH or immunohistochemistry for GluR2 have been reported in human striatum (Bernard et al., 1996, Meng et al., 1997; Cicchetti et al., 1999). In the present study, we found 1% of neurons in monkey striatum were ChAT+, as consistent with a previous report (DiFiglia, 1987), and they represented the largest neurons in rhesus striatum. Our data indicated that all

large striatal neurons in rhesus monkeys were weakly to moderately immunolabeled for GluR1, while about half each were immunolabeled for GluR2 and GluR4. The difference we observed in GluR2 and GluR2/3 expression in large striatal neurons suggested that about half of large-sized neurons may contain GluR3 but not GluR2. Our results thus suggest that cholinergic interneurons possess low to moderate levels of AMPA subunits, with GluR1 the most common subunit. Our previous immunolabeling studies and those of others reported that 69% of ChAT neuronal perikarya in rat striatum contain GluR1 and 55% contain GluR2. Further studies have reported that over 50% of cholinergic neurons in rat possess low levels of GluR3 and GluR4 (Bernard et al., 1996, 1997; Vorobjev et al., 2000).

Calretinergic Interneurons: CALR+ striatal interneurons possess medium-sized perikarya in rats (Bennett and Bolam, 1993a; Kawaguchi et al., 1995; Figueredo-Cardenas et al., 1996b; Deng et al., 2007), but include both large and medium-sized neurons in human and monkey striatum (Fortin and Parent, 1994; Prensa et al., 1998; Wu and Parent, 2000). It has been reported in human striatum that large CALR+ neurons co-contain ChAT (Cicchetti et al., 1999). Little is known of the physiology of striatal CALR+ neurons, but the medium-sized ones in rats are known to receive excitatory input that may be of cortical origin (Bennett and Bolam, 1993a). In the present study, we found that CALR+ neurons in rhesus constituted 9.1% of all neurons in caudate and 4.2% in putamen. The greater prevalence of CALR+ neurons in caudate than putamen that we observed in rhesus is consistent with a previous report on human and squirrel monkey (Wu and Parent, 2000). CALR+ neurons are also more abundant medially than laterally in rat striatum (Figueredo-Cardenas et al., 1996). Our 4.2–9.1% frequency for CALR+ striatal neurons, however, exceeds the 3% reported for human striatum (Parent et al., 1996; Prensa et al., 1998). This may be attributable to the better fixation and brain preservation generally possible with monkeys. Consistent with prior studies in primates, we did find that two types of perikarya were positive for CALR - one with medium-sized perikarya and the other with large perikarya. In our study, we found that large CALR+ neurons and large ChAT+ neurons make 0.3% and 1% of striatal neurons, respectively, indicating that 30% of ChAT neurons must contain CALR. Prior studies have reported that 60–90% of human striatal cholinergic neurons possess CALR (Massouh et al., 2008). Since we found that the large CALR+ neurons make up 30% of striatal cholinergic interneurons, our results imply that all large CALR+ striatal neurons in rhesus possess GluR1, and many or all possess GluR2 and/or GluR4 as well. Cicchetti et al. (1999) reported that about 50–60% of large CALR+ interneurons possess GluR1 and GluR2, while 50–70% contain GluR4 in human striatum.

The medium-sized CALR+ interneurons of rhesus striatum are likely to include both projection neurons and interneurons. Based on the frequency of ChAT+, SS+, and PARV+ interneurons and the frequency of striatal projection neurons indicated by our CALB immunolabeling, we estimate that CALR+ interneurons make up 1.5–2.0% of all striatal neurons in rhesus monkey. This type of interneuron has a yet lower frequency (<1%) in rats (Figueredo-Cardenas et al., 1996). Our data indicates also that about 7% of CALR+ caudate neurons and 2.5% of CALR+ putamen neurons in rhesus are projection neurons. The presence of CALR+ projection neurons in rhesus is consistent with prior evidence showing that some medium-sized CALR+ neurons in humans possess spiny dendrites and appear to be projection neurons (Prensa et al., 1998). Dendritic labeling of the CALR+ medium-sized was, however, not adequate for us to confirm that any in rhesus possessed spiny dendrites. Since the size of medium-sized CALR+ neurons overlaps that of projection neurons, our studies also do not allow us to reach conclusions on the AMPA receptor localization of medium-sized calretinergic neurons. Note that while CALB+, PARV+, and CALR+ neurons are all rich in calcium binding proteins, they are differentially affected in HD, with projection neurons and PARV interneurons vulnerable (Seto-Ohshima et al., 1988; Ferrer et al., 1994; Deng et al., 2004), and both the medium-sized CALR neurons and the large

cholinergic CALR+ interneurons resistant (Cichetti et al., 1996, 2000). It would be of interest to know if the CALR+ projection neurons constitute an HD-resistant group of striatal projection neurons, and thus account for the HD-resistance of medium-sized CALR neurons in humans.

Somatostatinergic Interneurons: SS+ striatal interneurons colocalize SS, NPY and NOS in their perikarya in primate and rodent (Smith and Parent, 1986; Figuerado-Cardenas et al., 1996a). Our finding that SS was found in medium-sized perikarya making up 1.5% of striatal neurons in monkey was congruent with previous reports (Wu and Parent, 2000). Striatal SS/NPY/NOS interneurons have been reported to receive minimal cortical input (Vuillet et al., 1989) and express only low levels of GluR1 and GluR2 in rats - 15% and 50%, respectively, of all striatal neurons (50% of all striatal neurons) (Catania et al., 1995; Kim et al., 2001; Deng et al., 2007). Since the size and shape of SS+ interneurons overlaps that of projection neurons, our studies do not allow us to reach firm conclusions on the extent of AMPA receptor localization in SS+ neurons in rhesus monkey striatum.

3.2 Implications for Striatal Neuron Function

The AMPA-mediated responses of neurons depend on not only the subunit composition of their AMPA receptors, but also their RNA editing, flip/flop isoforms, abundance, subsynaptic localization, association with TARPs, and phosphorylation state (Hollmann and Heinemann, 1994; Nicoll et al., 2006; Sager et al., 2009; Seeburg, 1993). With respect to editing, since R/G editing is about 80–90% complete in adult brain (Lomeli et al., 1994), R/G editing failure is unlikely to be a significant source of AMPA subunit variation among striatal neuron types. Similarly, RNA editing at the Q/R site of GluR2 is highly efficient in neonatal and adult brain, with only 1% of GluR2 subunits unedited (Carlson et al., 2000; Hollmann and Heinemann, 1994; Akbarian et al., 1995). Thus, it seems likely R/G and Q/R editing is relatively complete in monkey striatum. Prior quantitative immunohistochemical studies have shown that intensity of immunolabeling correlates with antigen level (Mize et al., 1988; Mize, 1994), and others have shown that amount of AMPA subunit message or protein in rodents is consistent with the observed neuronal physiology (Götz et al., 1997; Calabresi et al., 1998; Stefani et al., 1998; Vorobjev et al., 2000). Thus, the present findings on the frequency and abundance of specific AMPA subunits on specific types of striatal neurons have implications for their likely responses to corticostriatal and thalamostriatal inputs or glutamate. Receptor subsynaptic localization and phosphorylation state may also have an impact, but these were not assessed in the present study.

Electrophysiological studies in rodents have shown that striatal projection neurons show prominent AMPA receptor-mediated excitatory responses to cortical and thalamic input activation (Kita, 1996; Calabresi et al., 1998; Ding et al., 2008), which is consistent with the observed enrichment of rodent striatal projection neurons in AMPA subunits, especially the GluR1 and GluR2 subunits. Our observation that striatal projection neurons in rhesus are also enriched in GluR1 and GluR2 supports the interpretation that striatal projection neurons responses to cortical and thalamic input are likely to be GluR1/GluR2-mediated as well. While GluR2 subunits may predominate in striatal projection neuron perikarya in rodents (Deng et al., 2007), many projection neuron spines in rodents possess sufficient GluR2-lacking AMPA receptors to show some AMPA receptor-mediated Ca2+ influx (Carter and Sabatini, 2004). Our previous studies on AMPA subunit expression in rats indicated that GluR1 is more enriched in striato-GPe than striato-GPi and striatonigral neurons (Deng et al., 2007). Consistent with this, Kreitzer and Malenka (2007) found that AMPA receptors on ENK+ neurons show slightly greater rectification and thus Ca2+ entry than do SP+ neurons in rodents. It may be that the same is true in primates, and that the 14% of striatal neurons that are GluR1-rich projection neurons are mainly ENK+ striato-GPe neurons.

Parvalbuminergic interneurons have been shown to fire phasically at high frequency in response to cortical stimulation in rodents (Kawaguchi, 1993; Kita, 1993). While the high spike rate of this neuron upon depolarization appears to reflect an intrinsic membrane property, their relative enrichment in GluR1 and GluR4 compared to GluR2 in rodents (Tallaksen-Green and Albin, 1994; Chen et al., 1996; Bernard et al., 1997; Kwok et al., 1997; Deng et al., 2007) explains their inwardly rectifying I-V curve (Koos and Tepper, 1999), and indicates they are likely to mainly possess AMPA receptors with high calcium permeability (Geiger et al., 1995; Götz et al., 1997; Kondo et al., 1997; Washburn et al., 1997). The higher single-channel conductance and faster desensitization of GluR1/4-rich AMPA receptor may help explain the robust short duration action potential of PARV+ interneurons in response to cortical activation (Kawaguchi, 1993; Koos and Tepper, 1999). Given the current data also favor the enrichment of PARV+ interneurons in rhesus with GluR1 and GluR4, it seems likely that the AMPA physiology of this neuron type is as in rodents.

Cholinergic striatal interneurons receive limited excitatory input (Kawaguchi et al., 1995), which arises predominantly from thalamus (Lapper and Bolam, 1992), and accordingly have been found to be poorer in AMPA GluRs, and show weaker responses to cortical stimulation and AMPA agonists than projection neurons and PARV+ interneurons (Tallaksen-Green and Albin, 1994; Chen et al., 1996; Bernard et al., 1997; Kwok et al., 1997; Calabresi et al., 1998; Richardson et al., 2000; Deng et al., 2007). In rodents, however, striatal cholinergic neurons do possess some AMPA subunits, notably GluR1. This appears to explain why cholinergic interneurons show more rapid desensitization to AMPA agonists than do projection neurons (Götz et al., 1997; Washburn et al., 1997 Vorobjev et al., 2000). Since striatal cholinergic interneurons in rhesus monkey also are generally AMPA-poor but all possess GluR1, it seems likely that they too have weak but rapidly desensitizing AMPA responses.

Numerous authors have hypothesized that the AMPA receptor abundance and composition of neurons affects their vulnerability to excitotoxic injury, especially in the case of those striatal neurons that receive massive glutamatergic inputs (Schwarcz et al., 1984; Chen et al., 1995, 1999; Ikonomidou and Turski, 1996; Popoli et al., 2002). Studies of mice overexpressing the GluR2 subunit indicate that excitotoxic vulnerability increases as the abundance of AMPA receptors increases (Le et al., 1997). The observation that neurons rich in GluR1 and/or GluR4 subunits are more vulnerable than those equally rich in GluR2 indicates that lower GluR2 relative to GuR1/4 increases excitotoxic vulnerability (Pellegrini-Giampietro et al., 1992, 1997; Feldmeyer et al., 1999; Iihara et al., 2001; Van Den Bosch et al., 2000; Vandenberghe et al., 2000). Some studies have attributed this effect to the Ca^{2+} permeability of GluR2-deficient AMPA receptors (Van Den Bosch et al., 2000), while others have attributed it to the higher single channel conductance of GluR2-deficient AMPA receptors (Vandenberghe et al., 2000). Consistent with these various observations, preferential death of striatal projection neurons (GluR1/2-rich) and PARV+ interneurons (GluR1/4-rich) occurs in rodents after transient global ischemia or corticostriatally mediated excitotoxic injury (Beal. et al., 1986, 1991; Chesselet et al., 1990; DiFiglia, 1990; Uemura, et al., 1990; Figueredo-Cardenas, et al., 1994, 1997, 1998; Paschen, 1996; Meade et al., 2000). Striatal projection neurons in primates receive extensive glutamatergic input and we have found they express abundant AMPA receptors, as consistent with their preferential death in corticostriatally mediated excitotoxicity (Ferrante et al., 1993). The prominent responsiveness of PARV+ interneurons to cortical activation in monkeys (Parthasarathy and Graybiel, 1997), and their low GluR2 levels in conjunction with their enrichment in GluR1 and GluR4 yielding mainly Ca^{2+}-permeable AMPA receptors predicts that they should be vulnerable to excitotoxic injury and neurodegenerative disease in primates. The relatively low GluR1-GluR4 levels in ChAT+ and large CALR+ interneurons and their sparse cortical

input (Lapper and Bolam, 1992) suggests they, by contrast, should have low vulnerability to excitotoxicity (Ferrante et al., 1993). Further studies in primates are needed to determine if these striatal neuron types respond to ischemic or excitotoxic injury as predicted from their AMPA subunit profile.

Finally, some authors have also noted that AMPA-rich striatal neurons are vulnerable in Huntington's disease (HD), while AMPA-poor neurons are resistant, and on this basis suggested that AMPA receptor-mediated excitotoxicity may be involved in HD pathogenesis (Tallaksen-Green and Albin, 1994; Chen et al., 1995, 1996). Mutant mouse models, however, have implicated enhanced NMDA receptor sensitivity in HD (Song et al., 2003; Fan and Raymond, 2007), and evaluation of a role of AMPA receptors needs to consider the impact of disease on AMPA subunit RNA editing, protein production, posttranslational modification, and synaptic localization (Akbarian et al., 1995), which may render the role of AMPA receptors different in HD than in global ischemia or excitotoxicity. A role of AMPA receptors in HD pathogenesis, however, cannot be discounted, since NMDA receptor antagonist clinical trials have not shown significant benefit (Fan and Raymond, 2007).

4. Experimental procedures

4.1 Experimental Subjects

We carried out immunohistochemical studies to determine the localization of AMPA receptor subunits in striatum of rhesus monkey. Three adult rhesus monkeys (*Macaca Mulatta*) weighing between 5 and 10kg were used. Animal use was carried out in accordance with the National Institutes of Health *Guide for the Care and Use of Laboratory Animals*, Society for Neuroscience Guidelines, and the University of Alabama at Birmingham and University of Tennessee Health Science Center Guidelines.

4.2 Light Microscopic Immunohistochemical Single-Label Studies

Monkey brain tissue used in this study was provided by Dr. Paul D.R. Gamlin of the University of Alabama at Birmingham. Rhesus monkeys were deeply anesthetized with sodium pentobarbital and transcardially perfused with 0.1M sodium phosphate buffer (PB) (pH7.4) followed by 4% paraformaldehyde in 0.1M PB (pH 7.4). The brains were removed, post-fixed for 2–6 hours, and cryoprotected in a solution of 20% sucrose-10% glycerol-0.01 sodium azide in 0.1 M PB at 4°C. Transverse sections through the basal ganglia were cut frozen (50μm) on a sliding microtome, sequentially collected into 48 separate compartments, and stored at 4°C in 0.1M PB-0.01% sodium azide until processed for immunolabeling.

Following rinses in 0.1M PB, the free-floating sections were incubated at 4°C with slight agitation for 48–72 hours in anti-GluR1, anti-GluR2, anti-GluR2/3 or anti-GluR4 diluted with 5% normal goat serum - 0.3% Triton X-100 - 0.01% sodium azide in 0.1M PB (host species, dilution, sources and specificities for the GluR1-4 antibodies are listed in table 5). The antibodies for glutamate receptors were generated against synthetic fragments of rat AMPA subunits, with the anti-GluR2/3 recognizing an epitope common to rat GluR2 and GluR3. The anti-GluR antibodies are specific for their target antigens (table 5).

To relate GluR1-4 immunolabeled neurons to specific types of basal ganglia neurons by perikaryal size and shape, striatal neurons were immunolabeled for type-specific antigens, with immunolabeling for each antigen in a separate series of sections. Mouse anti-calbindin was used to characterize striatal projection neurons, although it should be noted that only projection neurons of the matrix compartment contain calbindin (CALB) and a small fraction of CALB+ striatal neurons appear to be aspiny interneurons (Gerfen et al., 1985; Bennett and Bolam, 1993b; Kubota et al., 1993). Striatal interneuron types were visualized

by immunolabeling for parvalbumin (PARV), calretinin (CALR), choline acetyltransferase (ChAT) or somatostatin (SS) (table 5). As noted above, many of the medium-sized CALR+ striatal neurons appear to be projection neurons. Finally, some sections were immunolabeled for the neuronal nuclear antigen (NeuN) to determine total neuron abundance in the striatum. The antibodies used to visualize these various basal ganglia neuron types, the dilutions used, their sources and their specificities are listed in table 5. For these primary antibody incubations as well, free-floating sections were incubated at 4°C with slight agitation for 48–72 hours in antibody diluted with 5% normal goat serum - 0.3% Triton X-100 - 0.01% sodium azide in 0.1M PB.

After incubation in the primary antibody, the sections were rinsed 3 times in 0.1M PB, incubated for 1–2 hours in donkey anti-rabbit, anti-mouse, or anti-goat antiserum (Jackson ImmunoResearch Labs, West Grove, PA) diluted 1:50, rinsed three times in 0.1M PB, and then incubated in a rabbit, mouse, or rat peroxidase-antiperoxidase (PAP) complex (Sternberger Monoclonals, Lutherville, MD) for 1–2 hours diluted 1:100. The secondary antisera and PAP were diluted in 0.1M PB containing 0.3% Triton X - 0.01% sodium azide, and the incubations were at room temperature with gentle agitation. Sections were then rinsed in 0.1M PB, the labeling visualized using diaminobenzidine tetrahydrochloride (DAB) as in our prior studies (Anderson and Reiner, 1991; Chen et al., 1996; Reiner et al., 1999; Deng et al., 2007), and the sections rinsed, mounted on gelatin-coated slides, dried, dehydrated, cleared with xylene and coverslipped with Permount®.

4.3 Analysis

All sections were examined using an Olympus BH-2 microscope, and illustrations shown here of this labeling were prepared digitally using Adobe Photoshop (v6.0). Contrast was enhanced, sharpness increased, and minor imperfections removed using the editing capabilities of this program.

4.3.1 Perikaryal Size Measurements—The mean perikaryal diameter was determined in caudate and putamen for neurons immunostained for GluR1, GluR2, GluR2/3, and GluR4. The sizes of CALB+, PARV+, CALR+, ChAT+, and SS+ perikarya were also measured to assist in matching specific cell types with neurons possessing specific types of AMPA subunits. To measure perikaryal size, random images of caudate and putamen for each marker were used, with the images captured digitally using a 20× objective on an Olympus BH-2 microscope, and analyzed using the public domain software NIH Image J. The perikaryal sizes of the neurons in these images were determined by measuring the long axes for each. To avoid including cellular fragments in the size determinations, the captured images were taken through a focal plane below the surface of the section. About 200 perikarya for each neuronal subtype were measured in random fields of caudate and putamen. A perikaryal size distribution histogram was then generated to compare the size range for each neuronal type (Fig. 4). Since all CALB and SS neurons were smaller than 19μm, while 98% of ChAT interneurons were ≥19μm, we categorized perikarya smaller than 19μm as medium-sized and those perikarya ≥19μm as large. While the size frequency histograms for CALB, ChAT, PARV and SS showed one main peak, that for CALR+ perikarya showed two clear peaks, one ≥19μm and one <19μm). We thus recognized two CALR+ neuron types: a large subgroup and a medium-sized subgroup. Since CALB+, ChAT+, PARV+, SS+ perikarya size distributions showed a single peak, we present the average diameter for each of these types without distinguishing between medium-sized and large perikarya. For CALR interneurons, we present separately the mean for the large and medium-sized subgroups. Since the perikarya immunolabeled for the AMPA subunits studied here also included large and medium-sized subgroups, we present the mean sizes for these subgroups as well.

4.3.2 Cell-type Abundance Determination—The abundance of neurons in caudate and putamen immunostained for GluR1, GluR2, GluR2/3, GluR4, CALB, PARV, CALR, ChAT, SS and NeuN was determined per unit area. For each case, labeled perikaryal abundance was determined in sixteen 400×400 μm^2 fields chosen at random for CALB, GluR1, GluR2, GluR2/3, and eight 400×400 μm^2 fields for NeuN, using an Olympus microscope with an eyepiece graticule. Twelve 1600×1600 μm^2 fields were chosen at random for measuring the abundance of ChAT+, PARV+, CALR+, SS+, and GluR4+ neurons, which were sparse. At least 400 of each neuron type were counted, and counts for each type were then corrected by the Abercrombie correction (Abercrombie, 1946). To express the frequency of each striatal neuron type as a percent of all striatal neurons, the areal abundance of each type was expressed as a percent of the areal abundance of those immunolabeled for NeuN (representing all striatal neurons). This approach suffices for our goal of establishing the relative abundance of striatal neuron types possessing specific GluRs (Saper, 1996).

Acknowledgments

We thank Aminah Henderson and Dr. Jian-Ping Xie for their excellent technical assistant. This research was supported by NS-19620, NS 28721 and NS-57722 (A.R.).

References

Abercrombie M. Estimation of nuclear population from microtome sections. Anat Rec. 1946; 94:239–247. [PubMed: 21015608]

Akbarian S, Smith MA, Jones EG. Editing for an AMPA receptor subunit RNA in prefrontal cortex and striatum in Alzheimer's disease, Huntington's disease and schizophrenia. Brain Res. 1995; 699:297–304. [PubMed: 8616634]

Anderson KD, Reiner A. Immunohistochemical localization of DARPP-32 in striatal projection neurons and striatal interneurons: implications for the localization of D1-like dopamine receptors on different types of striatal neurons. Brain Res. 1991; 568:235–243. [PubMed: 1839966]

Barden HJ. Interference filter microfluorometry of neuromelanin and lipofuscin in human brain. Neuropathol Exp Neurol. 1980; 39:598–605.

Beal MF, Kowall NW, Ellison DW, Mazurek MF, Swartz KJ, Martin JB. Replication of the neurochemical characteristics of Huntington's disease by quinolinic acid. Nature. 1986; 321:168–171. [PubMed: 2422561]

Beal MF, Ferrante RJ, Swartz KJ, Kowall NW. Chronic quinolinic acid lesions in rats closely resemble Huntington's disease. J Neurosci. 1991; 11:1649–1659. [PubMed: 1710657]

Bennett BD, Bolam JP. Characterization of calretinin-immunoreactive structures in the striatum of the rat. Brain Res. 1993a; 609:137–148. [PubMed: 8508297]

Bennett BD, Bolam JP. Two populations of calbindin D28k-immunoreactive neurones in the striatum of the rat. Brain Res. 1993b; 610:305–310. [PubMed: 8100472]

Bennett BD, Bolam JP. Localization of parvalbumin-immunoreactive structures in primate caudate-putamen. J Comp Neurol. 1994; 347:340–356. [PubMed: 7822489]

Bernard V, Gardiol A, Faucheux B, Bloch B, Agid Y, Hirsch EC. Expression of Glutamate receptors in the human and rat basal ganglia: effect of the dopaminergic denervation on AMPA receptor gene expression in the striatopallidal complex in Parkinson's disease and rat with 6-OHDA lesion. J Comp Neurol. 1996; 368:553–568. [PubMed: 8744443]

Bernard V, Somogyi P, Bolam JP. Cellular, subcellular, and subsynaptic distribution of AMPA-type glutamate receptor subunits in the neostriatum of the rat. J Neurosci. 1997; 17:819–833. [PubMed: 8987803]

Brizzee KR, Ordy JM, Kaack B. Early appearance and regional differences in intraneuronal and extraneuronal lipofuscin accumulation with age in the brain of a nonhuman primate (Macaca mulatta). J Gerontol. 1974; 29:366–81. [PubMed: 4209545]

Calabresi P, Centonze D, Pisani A, Sancesario G, Gubellini P, Marfia GA, Bernardi G. Striatal spiny neurons and cholinergic interneurons express differential ionotropic glutamatergic responses and vulnerability: Implications for ischemia and Huntington's disease. Ann Neurol. 1998; 43:586–597. [PubMed: 9585352]

Carlson NG, Howard J, Gahring LC, Roger SW. RNA editing (Q/R site) and flop/flip splicing of AMPA receptor transcripts in young and old brains. Neurobiol Aging. 2000; 21:599–606. [PubMed: 10924778]

Carter AG, Sabatini BL. State-dependent calcium signaling in dendritic spines of striatal medium spiny neurons. Neuron. 2004; 44:483–493. [PubMed: 15504328]

Catania MV, Tolle TR, Monyer H. Differential expression of AMPA receptor subunits in NOS-positive neurons of cortex, striatum, and hippocampus. J Neurosci. 1995; 15:7046–7061. [PubMed: 7472460]

Celio MR, Baier W, Scharer L, Gregersen HJ, de Viragh PA, Norman AW. Monoclonal antibodies directed against the calcium binding protein Calbindin D-28k. Cell Calcium. 1990; 11:599–602. [PubMed: 2285928]

Chen Q, Harris C, Brown CS, Howe A, Sumeier DJ, Reiner A. Glutamate-mediated excitotoxic death of cultured striatal neurons is mediated by non-NMDA receptors. Exp Neurol. 1995; 136:212–224. [PubMed: 7498411]

Chen Q, Veenman CL, Reiner A. Cellular expression of ionotropic glutamate receptor subunits on specific striatal neuron types and its implication for striatal vulnerability in glutamate receptor-mediated excitotoxicity. Neuroscience. 1996; 73:715–731. [PubMed: 8809793]

Chen Q, Veenman CL, Knopp K, Yan Z, Medina L, Song WJ, Surmeier DJ, Reiner A. Evidence for the preferential localization of GluR1 subunits of AMPA receptors to the dendritic spines of medium spiny neurons in rat striatum. Neuroscience. 1998; 83:749–761. [PubMed: 9483559]

Chen Q, Surmeier DJ, Reiner A. NMDA and non-NMDA receptor-mediated excitotoxicity are potentiated in cultured striatal neurons by prior chronic depolarization. Exp Neurol. 1999; 159:283–296. [PubMed: 10486197]

Chesselet MF, Lin CS, Polsky K, Jin BK. Ischemic damage in the striatum of adults gerbils: relative sparing of somatostatinergic and cholinergic interneurons contrasts with loss of efferent neurons. Exp Neurol. 1990; 110:209–218. [PubMed: 1977609]

Cicchetti F, Gould PV, Parent A. Sparing of striatal neurons coexpressing calretinin and substance P (NK-1) receptor in Huntington's disease. Brain Res. 1996; 730:232–237. [PubMed: 8883909]

Cicchetti F, Prensa L, Wu Y, Parent A. Chemical anatomy of striatal interneurons in normal individuals and in patients with Huntington's disease. Brain Res Rev. 2000; 34:80–101. [PubMed: 11086188]

Cicchetti F, Vinet J, Beach TG, Parent A. Differential expression of alpha-amino-3-hydroxy-5-methyl—4-isoxazolepropionate receptor subunits by calretinin immunoreactive neurons in the human striatum. Neuroscience. 1999; 93:89–97. [PubMed: 10430473]

Côté PY, Sadikot AF, Parent A. Complementary distribution of calbindin D-28k and parvalbumin in the basal forebrain and midbrain of the squirrel monkey. Eur J Neurosci. 1991; 3:1316–1329. [PubMed: 12106229]

Deng YP, Albin RL, Penney JB, Young AB, Anderson KD, Reiner A. Differential loss of striatal projection neurons in Huntington's disease: A quantitative immunohistochemical study. J Chem Neuroanatomy. 2004; 27:143–164.

Deng YP, Xie JP, Wang HB, Lei WL, Chen Q, Reiner A. Differential localization of the GluR1 and GluR2 subunits of the AMPA-type glutamate receptor among striatal neuron types in rats. J Chem Neuroanat. 2007; 32:167–192. [PubMed: 17446041]

Ding J, Peterson JD, Surmeier DJ. Corticostriatal and thalamostriatal synapses have distinctive properties. J Neurosci. 2008; 28:6483–6492. [PubMed: 18562619]

DiFiglia M. Synaptic organization of cholinergic neurons in the monkey neostriatum. J Comp Neurol. 1987; 255:245–258. [PubMed: 3819015]

DiFiglia M. Excitotoxic injury of the striatum: a model for Huntington's disease. Trends Neurosci. 1990; 13:286–289. [PubMed: 1695405]

Fan MMY, Raymond RA. N-Methyl-D-aspartate (NMDA) receptor function and excitotoxicity in Huntington's disease. Progress Nerobiol. 2007; 81:272–293.

Feldmeyer D, Kask K, Brusa R, Kornau HC, Kolhekar R, Rozov A, Burnashev N, Jensen V, Hvalby O, Spremgel R, Seeburg PH. Neurological dysfunctions in mice expressing different levels of the Q/R site-edited AMPAR subunit BluR-B. Nat Neurosci. 1999; 1:57–64. [PubMed: 10195181]

Ferrante RJ, Kowall NW, Cipolloni PB, Storey E, Beal MF. Excitotoxin lesions in primates as a model for Huntington's disease: histopathologic and neurochemical characterization. Exp Neurol. 1993; 119:46–71. [PubMed: 8432351]

Ferrer I, Kulisevsky J, Gonzalez G, Escartin A, Chivite A, Casas R. Parvalbumin-immunoreactive neurons in cerebral cortex and striatum in Huntington's disease. Neurodegeneration. 1994; 3:169–173.

Figueredo-Cardenas G, Anderson KD, Chen Q, Veenman CL, Reiner A. Relative survival of striatal projection neurons and interneurons after intrastriatal injection of quinolinic acid in rats. Exp Neurol. 1994; 129:37–56. [PubMed: 7925841]

Figueredo-Cardenas G, Morello M, Sancesario G, Bernardi G, Reiner A. Colocalization of somatostatin, neuropeptide Y, neuronal nitric oxide synthase and NADPH-diaphorase in striatal interneurons in rats. Brain Res. 1996a; 735:317–324. [PubMed: 8911672]

Figueredo-Cardenas G, Medina L, Reiner A. Calretinin is localized to a unique population of striatal interneurons in rats. Brain Res. 1996b; 709:145–150. [PubMed: 8869567]

Figueredo-Cardenas G, Chen Q, Reiner A. Age-dependent differences in survival of striatal somatostatin-NPY-NADPH-diaphorase-containing interneurons versus striatal projection neurons after intrastriatal injection of quinolinic acid in rats. Exp Neurol. 1997; 146:444–457. [PubMed: 9270055]

Figueredo-Cardenas G, Harris CL, Anderson KD, Reiner A. Relative resistance of striatal neurons containing calbindin or parvalbumin to quinolinic acid-mediated excitotoxicity compared to other striatal neuron types. Exp Neurol. 1998; 149:356–372. [PubMed: 9500958]

Fortin M, Parent A. Patches in the striatum of squirrel monkeys are enriched with calretinin fibers but devoid of calretinin cell bodies. Neurosci Lett. 1994; 182:51–54. [PubMed: 7891886]

Francois C, Yelnik J, Percheron G, Tande D. Calbindin D-28 as a marker for the associative cortical territory of the striatum in the macaque. Brain Res. 1994; 633:331–336. [PubMed: 8137167]

Geiger JRP, Melcher T, Koh DS, Sakmann B, Seeburg PH, Jonas P, Monyer H. Relative abundance of subunit mRNA determines gating and ca2+ permeability of AMPA receptors in principal neurons and interneurons in the rat CNS. Neuron. 1995; 15:193–204. [PubMed: 7619522]

Gerfen CR. The neostriatal mosaic: multiple levels of compartmental organization in the basal ganglia. Ann Rev Neurosci. 1992; 15:285–320. [PubMed: 1575444]

Gerfen CR, Baimbridge KG, Miller JJ. The neostriatal mosaic: compartmental distribution of calcium-binding protein and parvalbumin in the basal ganglia of the rat and monkey. Proc Natl Acad Sci U S A. 1985; 82:8780–8784. [PubMed: 3909155]

Gertler TS, Chan CS, Surmeier DJ. Dichotomous anatomical properties of adult striatal medium spiny neurons. J Neurosci. 2008; 2:10814–10824. [PubMed: 18945889]

Götz T, Kraushaar U, Geiger J, Lubke J, Berger T, Jonas P. Functional properties of AMPA and NMDA receptors expressed in identified types of basal ganglia neurons. J Neurosci. 1997; 17:204–215. [PubMed: 8987749]

Hollmann M, Heinemann S. Cloned glutamate receptors. Ann Rev Neurosci. 1994; 17:31–10. [PubMed: 8210177]

Iihara K, Joo DT, Henderson J, Sattlaer R, Taverna FA, Lourensen S, Orser BA, Rodeer JC, Tymianski M. The influence of glutamate receptor 2 expression on excitotoxicity in GluR2 null mutant mice. J Neurosci. 2001; 21:2224–2239. [PubMed: 11264298]

Ikonomidou C, Turski L. Neurodegenerative disorders: clues from glutamate and energy metabolism. Crit Rev Neurobiol. 1996; 10:239–263. [PubMed: 8971131]

Izzo PN, Graybiel AM, Bolam JP. Characterization of substance P- and [met]enkephalin-immunoreactive neurons in the caudate nucleus of cat and ferret by a single section Golgi procedure. Neuroscience. 1987; 20:577–587. [PubMed: 2438593]

Jonas P, Burnashev N. Molecular mechanisms controlling calcium entry through AMPA-type glutamate receptor channels. Neuron. 1995; 15:987–990. [PubMed: 7576666]

Kawaguchi Y. Physiological, morphological, and histochemical characterization of three classes of interneurons in rat neostriatum. J Neurosci. 1993; 13:4908–4923. [PubMed: 7693897]

Kawaguchi Y, Wilson CJ, Augood SJ, Emson PC. Striatal interneurons: chemical, physiological and morphological characterization. Trends Neurosci. 1995; 18:527–535. [PubMed: 8638293]

Keinanen K, Wisden W, Sommer B, Werner P, Herb A, Verdoorn TA, Sakamann B, Seeberg PH. A family of AMPA-selective glutamate receptors. Science. 1990; 249:556–560. [PubMed: 2166337]

Kim DY, Kim SH, Choi HB, Min C, Gwag BJ. High abundance of GluR1 mRNA and reduced Q/R editing of GluR2 mRNA in individual NADPH-diaphorase neurons. Mol Cell Neurosci. 2001; 17:1025–1033. [PubMed: 11414791]

Kita H. GABAergic circuits of the striatum. Prog Brain Res. 1993; 99:51–72. [PubMed: 8108557]

Kita H, Kosaka T, Heizmann CW. Parvalbumin-immunoreactive neurons in the rat neostriatum: a light and electron microscopic study. Brain Res. 1990; 536:1–15. [PubMed: 2085740]

Kondo M, Sumino R, Okado H. Combinations of AMPA subunit expression in individual cortical neurons correlate with expression of specific calcium-binding proteins. J Neurosci. 1997; 17:1570–1581. [PubMed: 9030617]

Koos T, Tepper JM. Inhibitory control of neostriatal projection neurons by GABAergic interneurons. Nature Neurosci. 1999; 2:467–472. [PubMed: 10321252]

Kubota Y, Mikawa S, Kawaguchi Y. Neostriatal GABAergic interneurones contain NOS, calretinin or parvalbumin. Neuroreport. 1993; 5:205–208. [PubMed: 7507722]

Kreitzer AC, Malenka RC. Endocannabinoid-mediated rescue of striatal LTD and motor deficits in Parkinson's disease models. Nature. 2007; 445:643–647. [PubMed: 17287809]

Kwok KHH, Tse YC, Wong RNS, Yung KKL. Cellular localization of GluR1, GluR2/3 and GluR4 glutamate receptor subunits in neurons of the rat neostriatum. Brain Res. 1997; 778:43–55. [PubMed: 9462876]

Lapper SR, Bolam JP. Input from the frontal cortex and the parafascicular nucleus to cholinergic interneurons in the dorsal striatum of the rat. Neuroscience. 1992; 51:533–545. [PubMed: 1488113]

Lapper SR, Smith Y, Sadikot AF, Parent A, Bolam JP. Cortical input to parvalbumin-immunoreactive neurones in the putamen of the squirrel monkey. Brain Res. 1992; 580:215–224. [PubMed: 1504801]

Le D, Das S, Wang YF, Yoshizawa T, Sasaki YF, Takasu M, Nemes A, Mendelsohn M, Dikkes P, Lipton SA, Nakanishi N. Enhanced neuronal death from focal ischemia in AMPA-receptor transgenic mice. Mol Brain Res. 1997; 52:235–241. [PubMed: 9495544]

Lei WL, Jiao Y, Del Mar N, Reiner A. Evidence for differential cortical input to direct pathway versus indirect pathway striatal projection neurons in rats. J Neurosci. 2004; 24:8289–8299. [PubMed: 15385612]

Lomeli H, Mosbacher J, Melcher T, Hoger T, Geiger JR, Kuner T, Monyer H, Higuchi M, Bach A, Seeburg PH. Control of kinetic properties of AMPA receptor channels by nuclear RNA editing. Science. 1994; 266:1709–1713. [PubMed: 7992055]

Martin LJ, Blackstone CD, Huganir RL, Price DL. The striatal mosaic in primates: striasomes and matrix are differentially enriched in ionotropic glutamate receptor subunits. J Neurosci. 1993a; 13:782–792. [PubMed: 7678861]

Martin LJ, Blackstone CD, Levey AI, Huganir RL, Price DL. AMPA glutamate receptor subunits are differentially distributed in rat brain. Neuroscience. 1993b; 53:327–358. [PubMed: 8388083]

Massouh M, Wallman MJ, Pourcher E, Parent A. The fate of the large striatal interneurons expressing calretinin in Huntington's disease. Neurosci Res. 2008; 62:216–224. [PubMed: 18801393]

Mayer ML, Armstrong N. Structure and function of glutamate receptor ion channels. Ann Rev Physiol. 2004; 66:161–81. [PubMed: 14977400]

Meade CA, Figueredo-Cardenas G, Fusco F, Nowak TS Jr, Pulsinelli WA, Reiner A. Transient global ischemia in rats yields striatal projection neuron and interneuron loss resembling that in Huntington's disease. Exp Neurol. 2000; 166:307–323. [PubMed: 11085896]

Meng SZ, Obonai T, Isumi H, Takashima S. A developmental expression of AMPA-selective glutamate receptor subunits in human basal ganglia. Brain and Development. 1997; 19:388–392. [PubMed: 9339865]

Mize RR. Quantitative image analysis for immunocytochemistry and *in situ* hybridization. J Neurosci Meth. 1994; 54:219–237.

Mize RR, Holdefer RN, Nabors LB. Quantitative immunocytochemistry using an image analyzer. I. Hardware evaluation, image processing, and data analysis. J Neurosci Meth. 1988; 26:1–24.

Mullen RJ, Buck CR, Smith AM. NeuN, a neuronal specific nuclear protein in vertebrates. Development. 1992; 116:201–211. [PubMed: 1483388]

Nicoll RA, Tomita S, Bredt DS. Auxiliary subunits assist AMPA-type glutamate receptors. Science. 2006; 311:1253–1256. [PubMed: 16513974]

Paquet M, Smith Y. Differential localization of AMPA glutamate receptor subunits in the two segments of the globus pallidus and the substantia nigra pars reticulata in the squirrel monkey. Eur J Neurosci. 1996; 8:229–233. [PubMed: 8713467]

Parent A, Fortin M, Cote P-Y, Cicchetti F. Calcium-binding proteins in primate basal ganglia. Neuroscience Res. 1996; 25:309–334.

Parthasarathy HB, Graybiel AM. Cortically driven immediate-early gene expression reflects modular influence of sensorimotor cortex on identified striatal neurons in the squirrel monkey. J Neurosci. 1997; 17:2477–2491. [PubMed: 9065508]

Paschen W. Glutamate excitotoxicity in transient global cerebral ischemia. Acta Neurobiol Exp. 1996; 56:313–322.

Pellegrini-Giampietro DE, Gorter JA, Bennett MVL, Zukin RS. The GluR2(GluR-B) hypothesis:Ca2+-permeable AMPA receptors in neurological disorders. Trends Neurosci. 1997; 20:464–470. [PubMed: 9347614]

Pellegrini-Giampietro DE, Zukin RS, Bennett MV, Cho S, Pulsinelli WA. Switch in glutamate receptor subunit gene expression in CA1 subfield of hippocampus following global ischemia in rats. Proc Natl Acad Sci USA. 1992; 89:10499–10503. [PubMed: 1438239]

Petralia RS, Wenthold RJ. Light and electron immunocytochemical localization of AMPA-selective glutamate receptors in the rat brain. J Comp Neurol. 1992; 318:329–354. [PubMed: 1374769]

Popoli P, Pintor A, Domenici MR, Frank CM, Rebano T, Pezzola A, Scarchilli L, Quarta D, Reggio R, Malchiodi-Albedi F, Falchi M, Massotti M. Blockade of striatal Adenosine A_{2A} receptor reduces, through a presynatpic mechanism, quinolinic acid-induced excitotoxicity: Possible relevance to neuroprotective interventions in neurodegenerative disease of the striatum. J Neurosci. 2002; 22:1967–1975. [PubMed: 11880527]

Prensa L, Gimenez-Agaya JM, Parent A. Morphological features of neurons containing calcium-binding proteins in the human striatum. J Comp Neurol. 1998; 390:552–563. [PubMed: 9450535]

Reiner A, Medina L, Haber SN. The distribution of dynorphinergic terminals in striatal target regions in comparison to the distribution of substance P-containing and enkephalinergic terminals in monkeys and humans. Neuroscience. 1999; 88:775–793. [PubMed: 10363817]

Reiner A, Jiao Y, Del Mar N, Laverghetta AV, Lei WL. Differential morphology of pyramidal-tract type and intratelencephalically-projecting type corticostriatal neurons and their intrastriatal terminals in rats. J Comp Neurol. 2003; 457:420–440. [PubMed: 12561080]

Rymar VV, Sasseville R, Luk KC, Sadikot AF. Neurogenesis and stereological morphomery of calretinin-immunoreactive GABAergic interneurons of the neostriatum. J Comp Neurol. 2004; 469:325–339. [PubMed: 14730585]

Richardson PJ, Dixon AK, Lee K, Bell MI, Cox PJ, Williams R, Pinnock RD, Freeman TC. Correlating physiology with gene expression in striatal cholinergic neurones. J Neurochem. 2000; 74:839–846. [PubMed: 10646537]

Sager C, Tapken D, Kott S, Hollmann M. Functional modulation of AMPA receptors by transmembrane AMPA receptor regulatory proteins. Neuroscience. 2009; 158:45–54. [PubMed: 18304745]

Santos SD, Carvalo AL, Caldeira MV, Duarte CB. Regulation of AMPA receptors and synaptic plasticity. Neuroscience. 2009; 158:105–125. [PubMed: 18424006]

Saper CB. Any way you cut it: A new journal policy for the use of unbiased counting methods. J Comp Neurol. 1996; 364:5. [PubMed: 8789271]

Schnell SA, Staines WA, Wessendorf MW. Reduction of lipofuscin-like autofluorescence in fluorescently labeled tissue. J Histochem Cytochem. 1999; 47:719–30. [PubMed: 10330448]

Schwarcz RAC, Foster ED, French WO, Whetsell, Kohler C. Excitoxic models for neurodegenerative disorders. Life Sci. 1984; 35:19–32. [PubMed: 6234446]

Seeburg PH. The molecular biology of mammalian glutamate receptor channels. Trends Neurosci. 1993; 16:359–65. [PubMed: 7694406]

Selemon LD, Goldman-Rakic PS. Longitudinal topography and interdigitation of corticostriatal projections in the rhesus monkey. J Neurosci. 1985; 5:776–794. [PubMed: 2983048]

Seto-Ohshima A, Emson PC, Lawson E, Mountjoy CQ, Carrasco LH. Loss of matrix calcium-binding protein-containing neurons in Huntington's disease. Lancet. 1988; 1(8597):1252–1255. [PubMed: 2897519]

Shiromani PJ, Armstrong DM, Bruce G, Hersh LB, Groves PM, Gillin JC. Relation of pontine choline acetyltransferase immunoreactive neurons with cells which increase discharge during REM sleep. Brain Res Bull. 1987; 18:447–455. [PubMed: 3580914]

Smith Y, Parent A. Neuropeptide Y-immunoreactive neurons in the striatum of cat and monkey: morphological characteristics, intrinsic organization and co-localization with somatostatin. Brain Res. 1986; 372:241–252. [PubMed: 2871900]

Smith Y, Raju DV, Pare JF, Sidibe M. The thalamostriatal system: a highly specific network of the basal ganglia circuitry. Trends Neurosci. 2004; 27:520–527. [PubMed: 15331233]

Smith Y, Charara A, Paquet M, Kieval JZ, Paré JF, Hanson JE, Hubert GW, Kuwajima M, Levey AI. Ionotropic and metabotropic GABA and glutamate receptors in primate basal ganglia. J Chem Neuroanat. 2001; 22:13–42. [PubMed: 11470552]

Snyder GL, Allen PB, Fienberg AA, Valle CG, Huganir CG, Nairn AC, Greengard P. Regulation of phosphorylation of the GluR1 AMPA receptor in the neostriatum by dopamine and psychostimulants *in vivo*. J Neurosci. 2000; 20:4480–4488. [PubMed: 10844017]

Somogyi P, Bolam JP, Smith AD. Monosynaptic cortical input and local axon collaterals of identified striatonigral neurons. A light and electron microscopic study using the Golgi-peroxidase transport-degeneration procedure. J Comp, Neurol. 1981; 195:567–584. [PubMed: 6161949]

Song C, Zhang Y, Parsons CG, Liu YF. Expression of polyglutamine-expanded huntingtin induces tyrosine phosphorylation of N-methyl-D-aspartate receptors. J Biol Chem. 2003; 278:33364–33369. [PubMed: 12810713]

Stefani A, Chen Q, Flores-Hernandez J, Jiao Y, Reiner A, Surmeier DJ. Physiological and molecular properties of AMPA/KA receptors expressed by striatal medium spiny neurons. Dev Neurosci. 1998; 20:242–252. [PubMed: 9691198]

Tallaksen-Greene SJ, Albin RL. Localization of AMPA-selective excitatory amino acid receptor subunits in identified populations of striatal neurons. Neuroscience. 1994; 61:509–519. [PubMed: 7969927]

Tomiyama M, Palacios JM, Cortés R, Vilaró MT, Mengod G. Distribution of AMPA receptor subunit mRNAs in the human basal ganglia: an in situ hybridization study. Mol Brain Res. 1997; 46:281–289. [PubMed: 9191103]

Uemura Y, Kowall NW, Beal MF. Selective sparing of NADPH-diaphorase-somatostatin-neuropeptide Y neurons in ischemic gerbil striatum. Ann Neurol. 1990; 27:620–625. [PubMed: 1972876]

Van Den Bosch L, Vandenberghe W, Klaassen H, Van Houtte E, Robberecht W. Ca2+-permeable AMPA receptors and selective vulnerability of motor neurons. J Neurol Sci. 2000; 180:29–34. [PubMed: 11090861]

Vandenberghe W, Robberecht W, Brorson JR. AMPA receptor calcium permeability, GluR2 expression, and selective motoneuron vulnerability. J Neurosci. 2000; 20:123–132. [PubMed: 10627588]

Vincent SR, Johansson O. Striatal neurons containing both somatostatin- and avian pancreatic polypeptide (APP)-like immunoreactivities and NADPH-diaphorase activity: a light and electron microscopic study. J Comp Neurol. 1983; 217:264–270. [PubMed: 6136532]

Vissavajjhala P, Janssen WGM, Hu Y, Gazzaley AM, Moran T, Hof PR, Morrison JH. Synaptic distribution of the AMPA-GluR2 subunit and its colocalization with calcium-binding proteins in rat cerebral cortex: an immunohistochemical study using a GluR2-specific monoclonal antibody. Exp Neurol. 1996; 142:296–312. [PubMed: 8934561]

Vorobjev VS, Sharonova IN, Haas HL, Sergeeva OA. Differential modulation of AMPA receptors by cyclothiazide in two types of striatal neurons. Eur J Neurosci. 2000; 12:2871–2880. [PubMed: 10971630]

Vuillet J, Kerkerian L, Kachidian P, Bosler O, Nieoullon A. Ultrastructural correlates of functional relationships between nigral dopaminergic or cortical afferent fibers and neuropeptide Y-containing neurons in the rat striatum. Neurosci Lett. 1989; 100:99–104. [PubMed: 2761790]

Washburn MS, Numberger M, Zhang S, Dingledine R. Differential dependence on GluR2 expression of three characteristic features of AMPA receptors. J Neurosci. 1997; 17:9393–9406. [PubMed: 9390995]

Wenthold RJ, Yokotani N, Doi K, Wada K. Immunochemical characterization of the non-NMDA glutamate receptor using subunit-specific antibodies. Evidence for a hetero-oligomeric structure in rat brain. J Biol Chem. 1992; 267:501–507. [PubMed: 1309749]

Wilson, CJ. The contribution of cortical neurons to the firing pattern of striatal spiny neurons. In: Houk, JC.; Davis, JL.; Beiser, DG., editors. Models of Information Processing in the Basal Ganglia. MIT Press; Cambridge, Massachusetts: 1995. p. 29-50.

Wu Y, Parent A. Striatal interneurons expressing calretinin, parvalbumin or NADPH-diaphorase: a comparative study in the rat, monkey and human. Brain Res. 2000; 863:182–191. [PubMed: 10773206]

Zimmermann L, Schwaller B. Monoclonal antibodies recognizing epitopes of calretinins: dependence on Ca2+-binding status and differences in antigen accessibility in colon cancer cells. Cell Calcium. 2002; 31:13–25. [PubMed: 11990296]

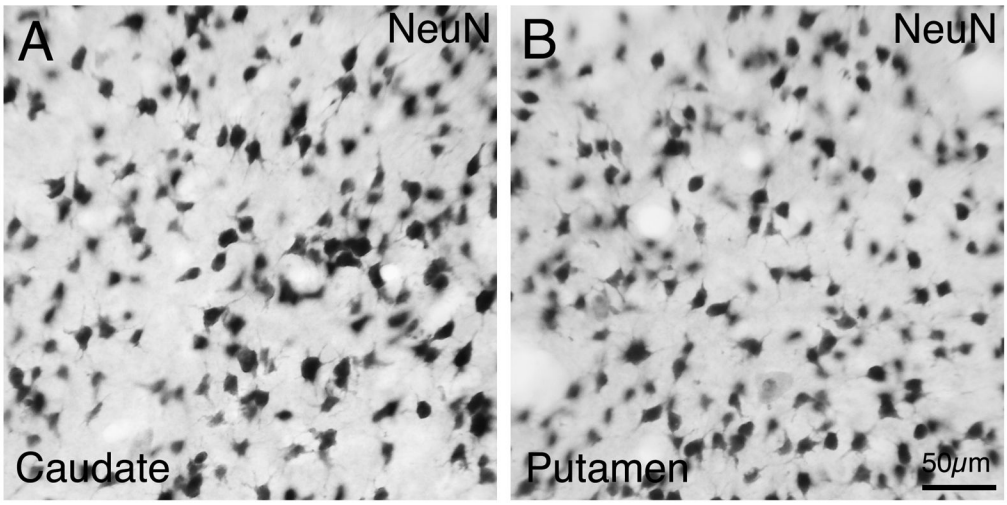

Fig. 1.
Images of NeuN-immunolabeled neurons in caudate (A) and putamen (B) of rhesus monkey. Scale bar = 50 μm. Magnification in A and B are the same.

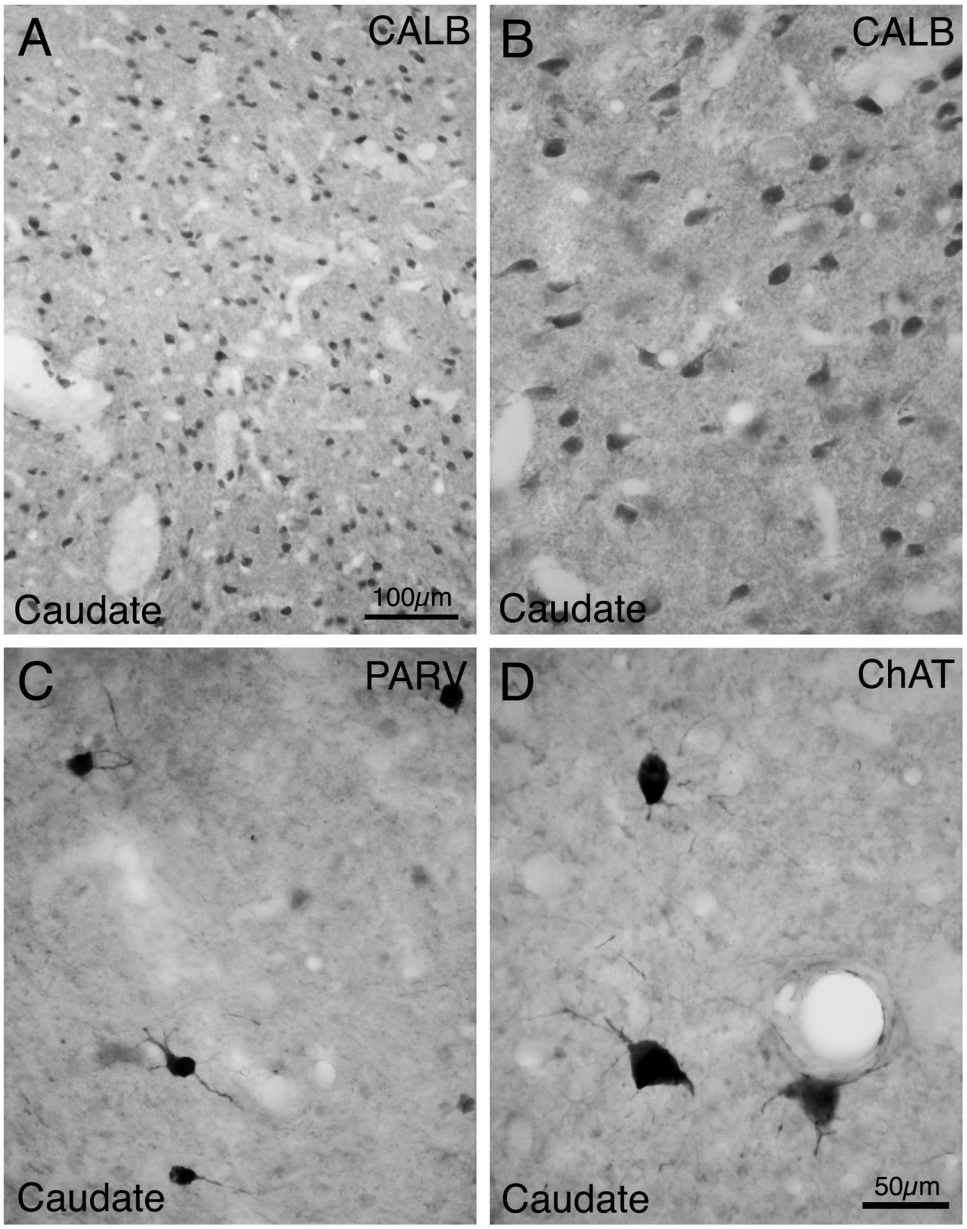

Fig. 2.

Images of neurons immunolabeled for CALB (A, B), PARV (C), and ChAT (D) in rhesus monkey striatum. Note that CALB+ neurons are medium-sized (A, low power; B, high power). PARV+ neurons are medium to large in size, and ChAT+ neurons are large, Immunolabeled primary dendrites are evident in both C and D. Magnification in B-D is the same.

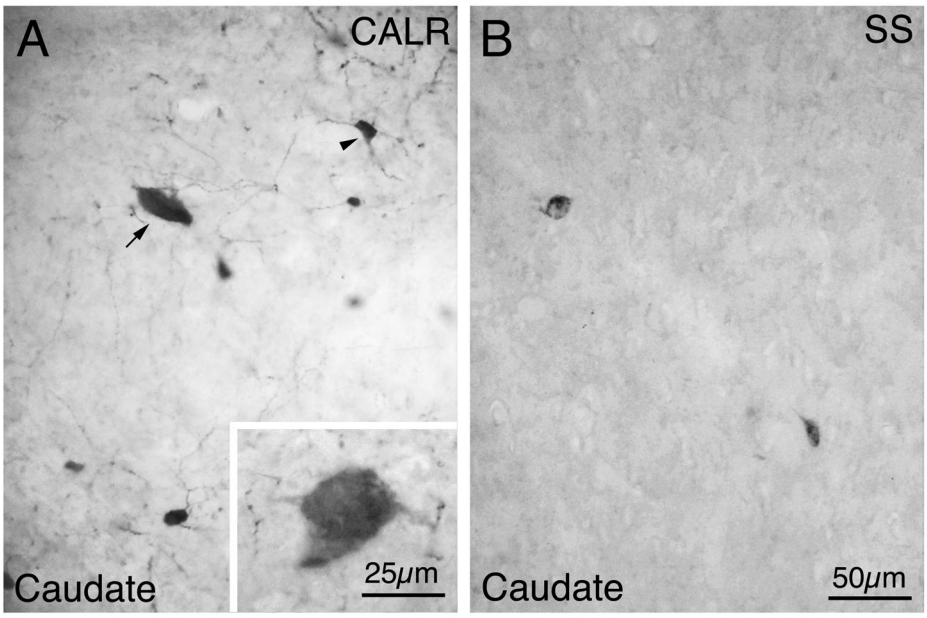

Fig. 3.

Images of neurons immunolabeled for CALR (A) and SS (B) in monkey striatum. Note that large neurons (arrow) and medium-sized neurons (arrowhead) are immunolabeled for CALR, but only medium-sized neurons are immunolabeled for SS. The inset in A shows a large CALR+ perikaryon with immunolabeled primary dendrites. Magnification in A and B are the same.

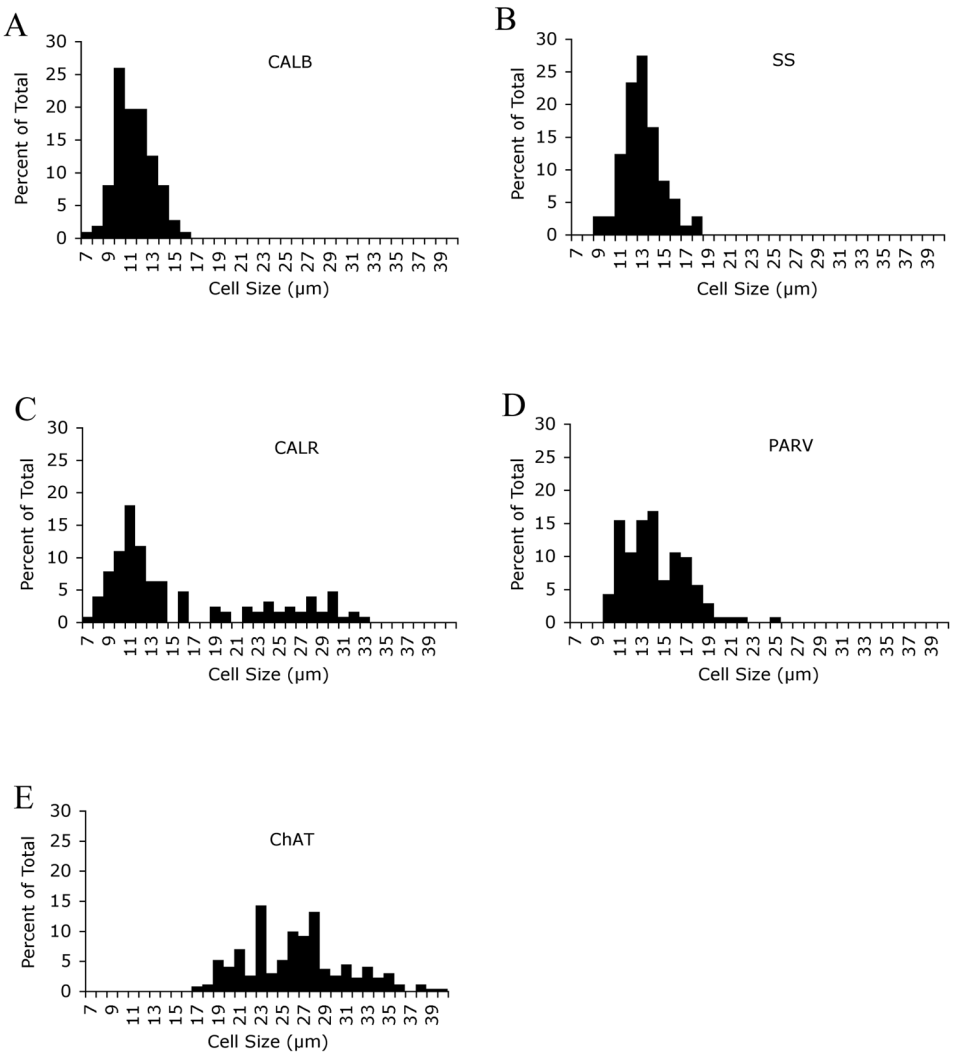

Fig. 4.

Frequency histograms for perikaryal size of striatal neurons immunolabeled for CALB (A), SS (B), CALR (C), PARV (D) and ChAT (E) in monkey caudate and putamen. About 200 perikarya for each marker were randomly measured in striatum. Note that CALB+, SS+, PARV+, and ChAT+ neuron size distributions are relatively narrow and largely with a single peak. The histograms show that the CALB+ and SS+ perikarya were medium-size, while PARV+ perikarya were medium to large-sized, and ChAT+ neurons were large (≥19μm). The CALR+ perikarya size distribution was broad and showed two peaks, indicating that CALR+ neurons included a medium-sized and a large-sized population. As noted in the text, the large CALR+ neurons represent a subset of the cholinergic striatal interneurons.

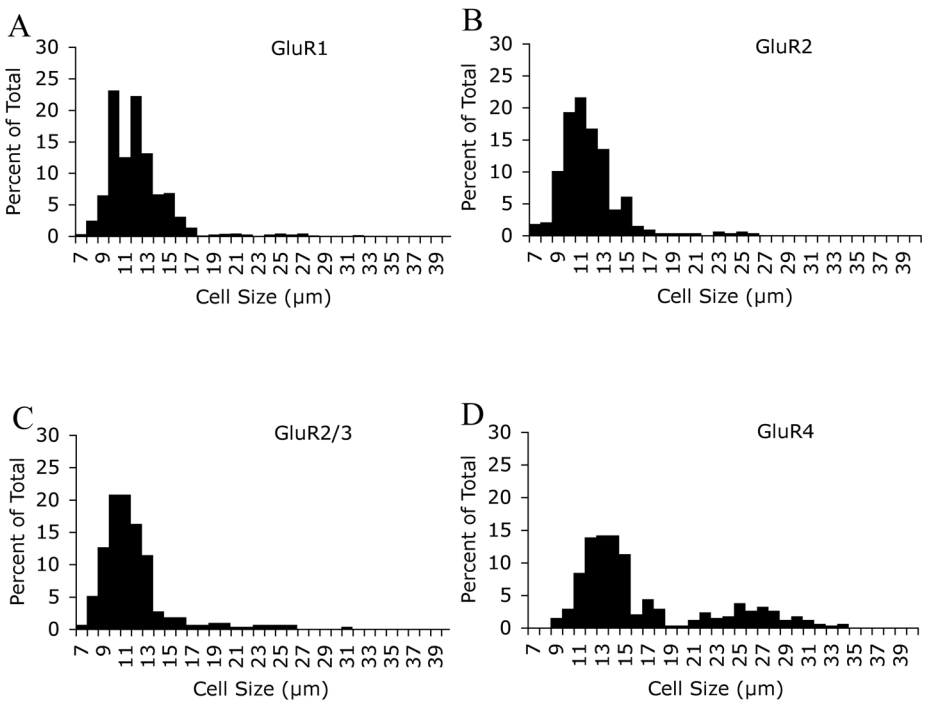

Fig. 5.

Frequency histograms for perikaryal size distribution of neurons immunolabeled for GluR1 (A), GluR2 (B), GluR2/3 (C), and GluR4 (D) in monkey caudate and putamen. About 200 perikarya for each subunit were randomly measured in striatum. Note that the AMPA subunits were found in both medium-sized and large neurons.

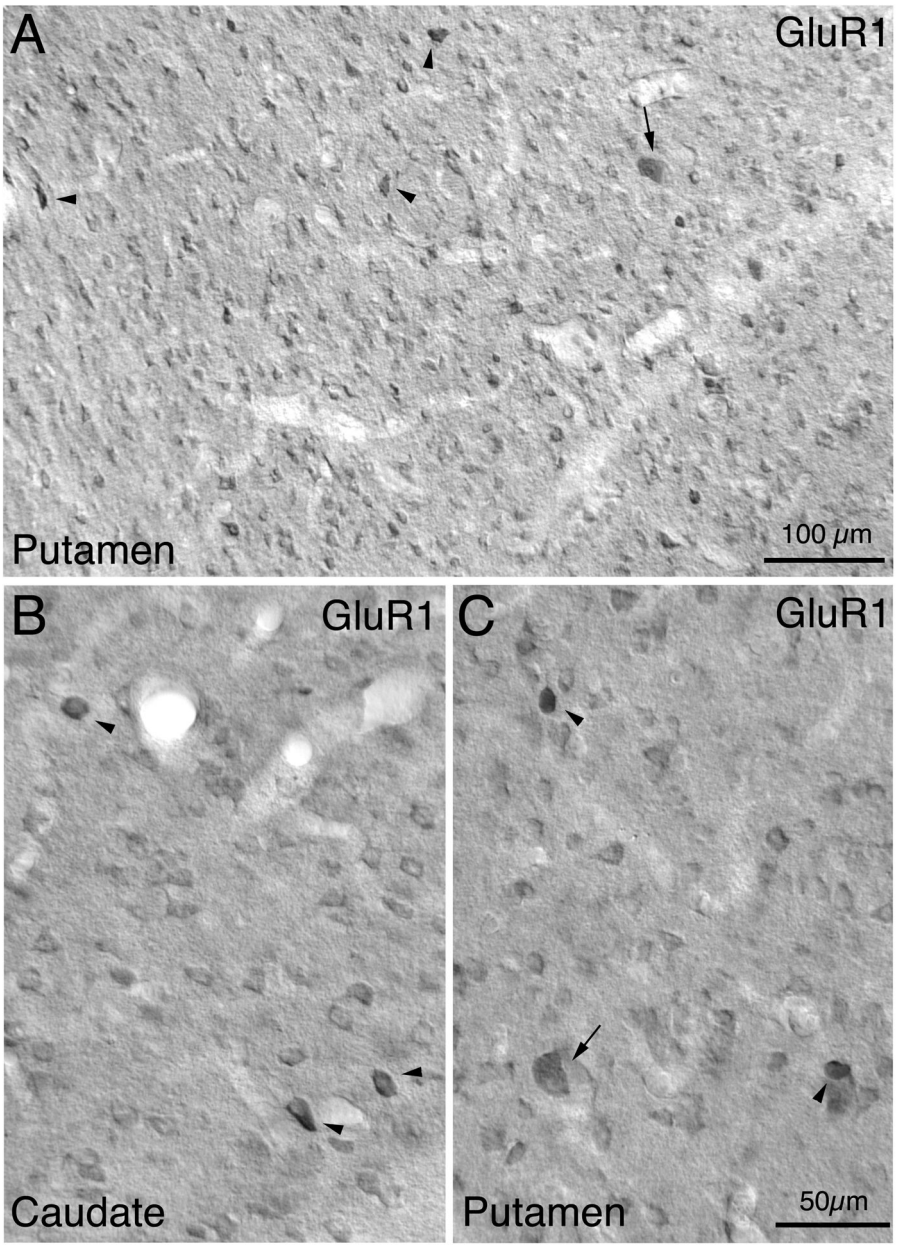

Fig. 6.

Low power (A) and high power (B, C) images of GluR1-immunolabeled neurons in monkey caudate (B) and putamen (A, C). Note that a sparse population of large neurons (arrow) and most of the medium-sized neurons are moderately immunolabeled. Some medium- to large-sized neurons are, however, intensely labeled for GluR1 (arrowhead). Magnification in B and C are the same.

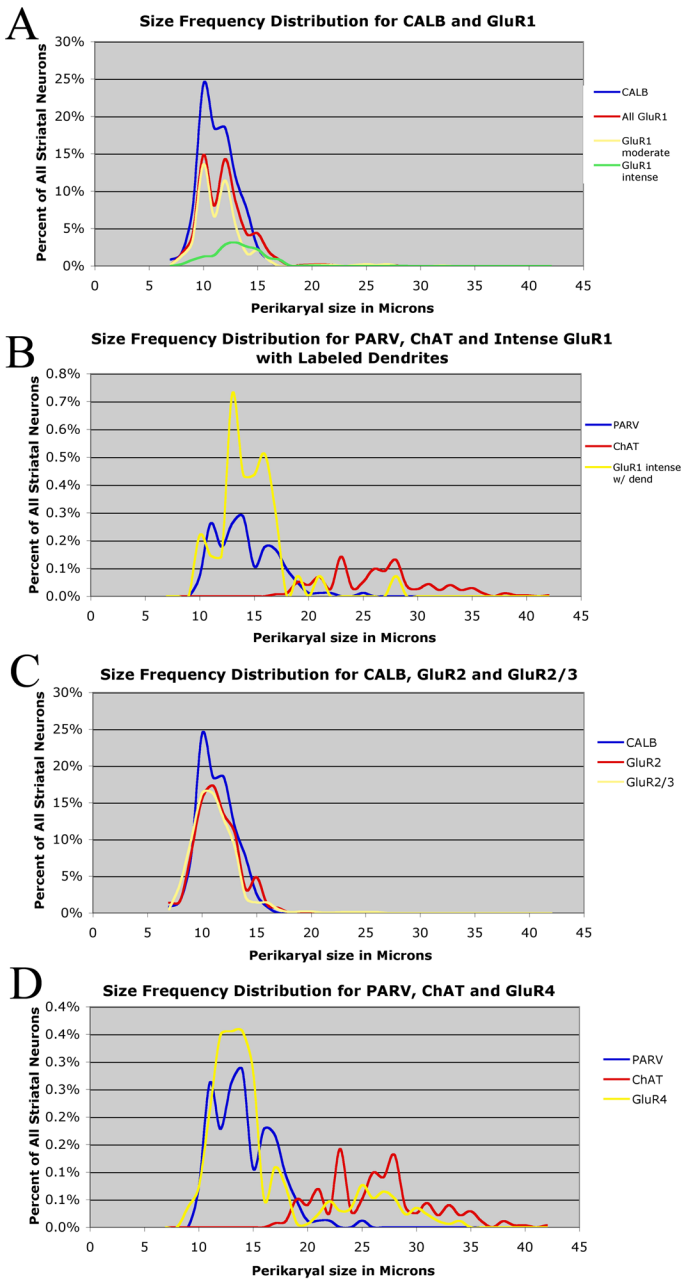

Fig. 7.

Comparison of size frequency histograms between immunolabeled striatal neuron types and specific GluRs. Graph A shows that the perikaryal size distribution of the CALB+ projection neurons matches that of the GluR1+ neurons, indicating that the vast majority of the GluR1+ perikarya are projection neurons. The size distributions for the moderately labeled and intensely labeled GluR1+ perikarya are shown separately, as is the distribution for all GluR1+ perikarya combined. Note that two GluR1 peaks are evident, aligning with apparent projection neuron peaks at 10μm and 12μm. Graph B shows the perikaryal size distributions for PARV+ and ChAT+ interneurons compared to that for the GluR1+ neurons that are intensely labeled and possess dendrites. Note that the PARV+ neuron size distribution closely matches the size distribution of GluR1+ neurons that are intensely labeled and

possess dendrites, indicating that all PARV+ neurons are likely to be GluR1-rich in rhesus. Graph C shows that the perikaryal size distribution of the CALB+ projection neurons matches that of the GluR2+ neurons and GluR2/3+ neurons, indicating that the vast majority of the GluR2+ and GuR2/3+ perikarya are projection neurons. Graph D shows that the perikaryal size distribution of the PARV+ and ChAT+ neurons compared to that for the GluR4+ neurons. Note the close match of the GluR4 distribution to the PARV+ neuron distribution, and the overlap of the GluR4 and ChAT distributions, indicating that the vast majority of the PARV+ neurons possess GluR4, and about half of the ChAT neuron do.

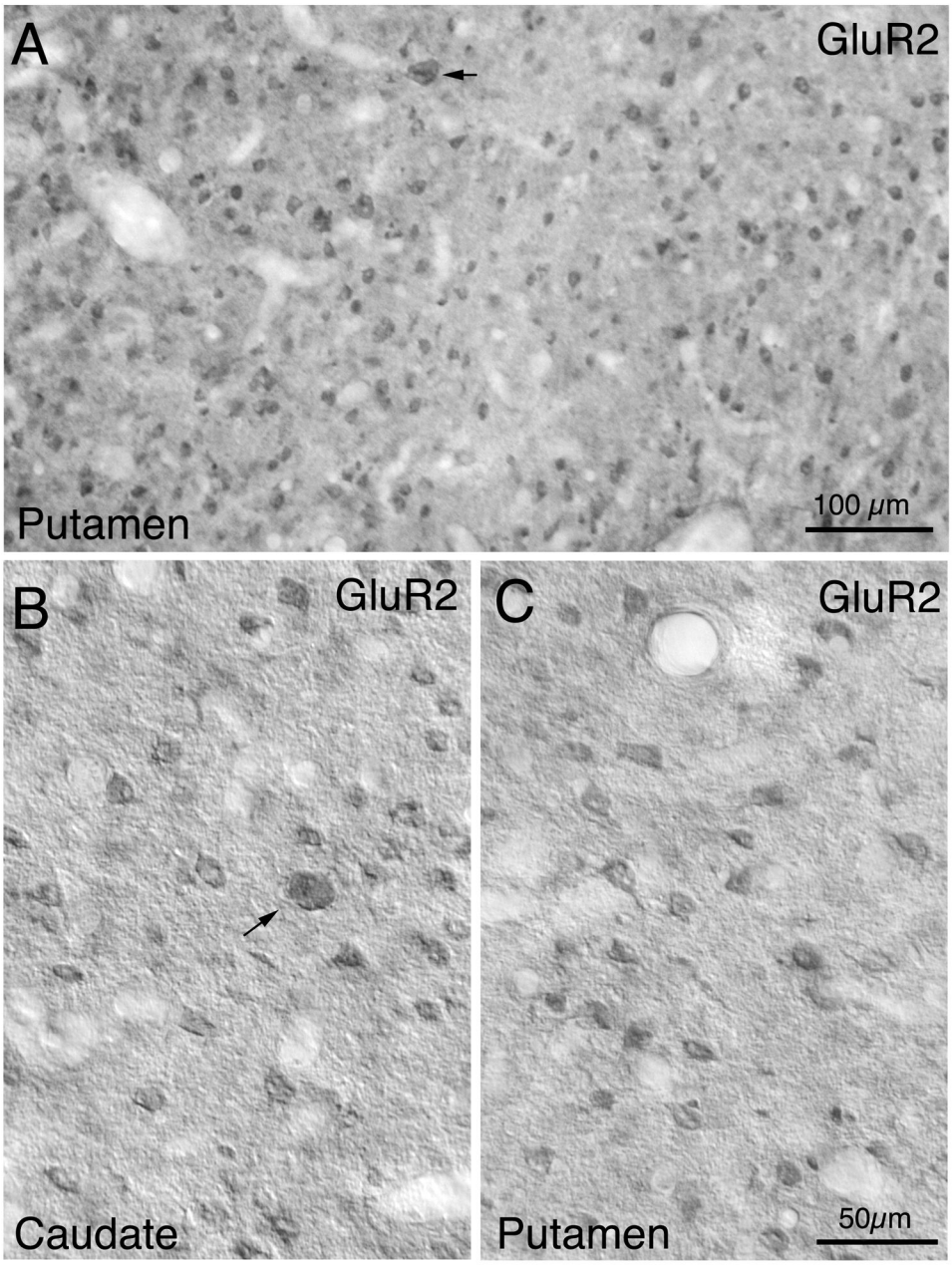

Fig. 8.

Low power (A) and high power (B, C) images of GluR2-immunolabeled neurons in monkey caudate (B) and putamen (A, C). Note that a sparse population of large neurons (arrow) and numerous medium-sized neurons are labeled. Notably pale streaks in A represent fiber bundles. Magnification in B, C are the same.

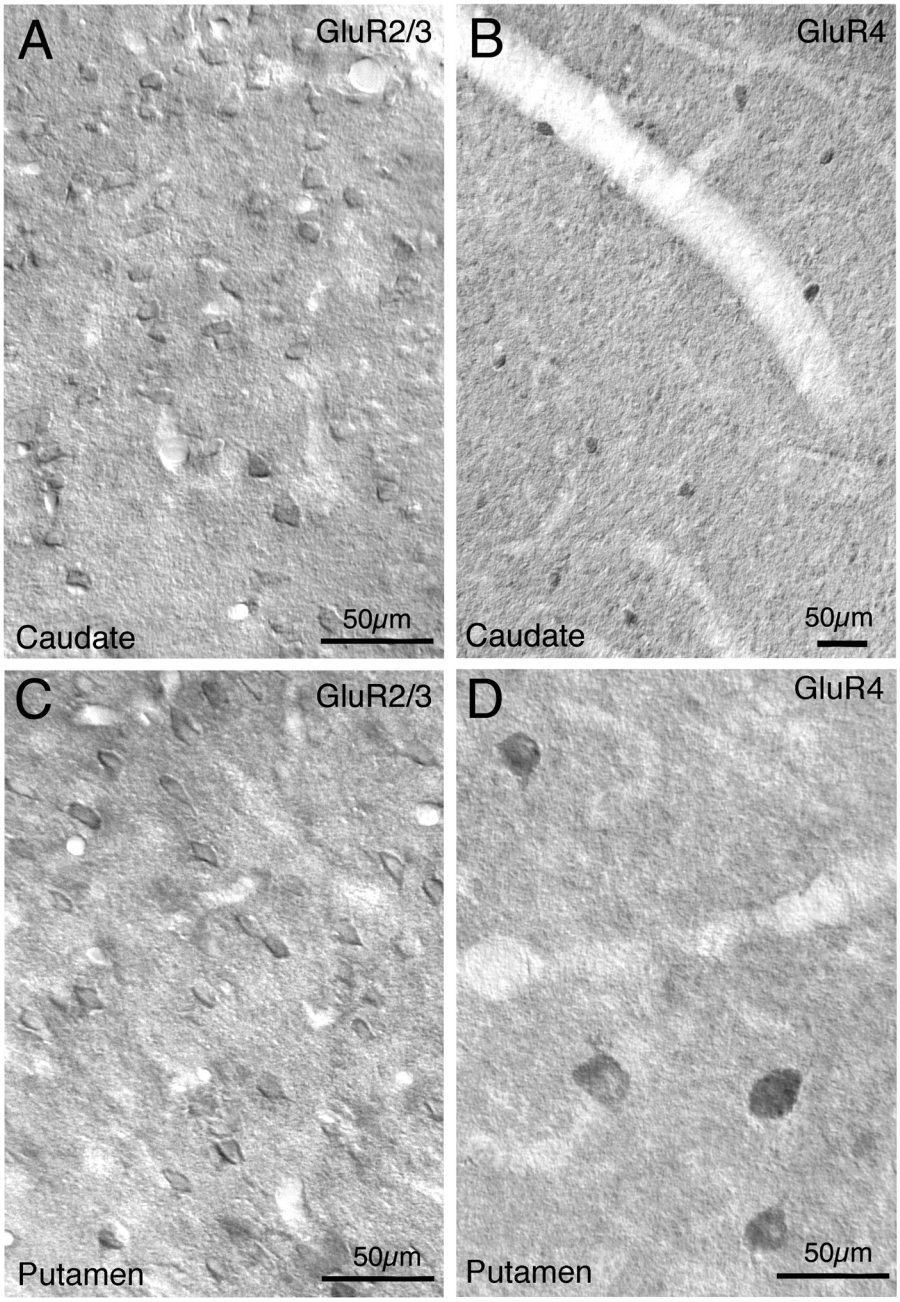

Fig. 9.

Images of GluR2/3-immunolabeled (A, C) and GluR4+ (B, D) neurons in monkey striatum. Note that numerous striatal neurons are labeled for GluR2/3, while only sparse medium-sized to large neurons are labeled for GluR4. Notably pale streaks in A represent fiber bundles. Magnification in A, C, and D are the same.

Table 1
Size of Immunolabeled Striatal Perikarya in Monkey

Perikaryal size of neurons immunolabeled for striatal neuronal markers and AMPA subunits in caudate and putamen of rhesus monkey. The immunolabeling for some AMPA units and neuron types are divided into subcategories based on their staining intensity and/or perikaryal size (large ≥19μm; medium-sized <19μm). Sizes are expressed as mean ± SD

Marker	Labeled Perikarya Categories	Caudate (μm)	Putamen (μm)	Combined (μm)
CALB	All	11.3±1.5 (matrix)	11.4±1.9 (striosome+matrix)	11.4±1.7
CHAT	All	26.5±4.8	26.7±4.8	26.6±4.8
PARV	All	15.0±3.0	14.2±2.7	14.3±2.8
CALR	Large (≥19μm)	25.4±3.8	26.4±4.0	26.1±4.0
CALR	Medium-sized (<19μm)	10.9±1.9	11.9±2.1	11.4±2.1
SS	All	13.0±1.5	13.1±2.1	13.0±1.8
GluR1	Large (≥19μm) (moderately labeled)	25.5±4.1	24.3±3.5	25.1±4.0
GluR1	Medium-sized (<19μm) (moderately labeled)	10.4±1.0	10.9±1.0	10.6±1.0
GluR1	Medium-sized (<19μm) (intensely labeled)	12.6±2.2	12.9±1.8	12.8±2.0
GluR1	Large (≥19μm) (intensely labeled)	22.6±3.1	21.6±1.7	22.0±2.3
GluR2	Large (≥19μm)	23.7±2.6	24.7±3.9	24.2±3.3
GluR2	Medium-sized (<19μm)	11.0±1.7	10.6±1.7	10.7±1.6
GluR2/3	Large (≥19μm)	23.4±2.2	23.3±2.3	23.3±2.2
GluR2/3	Medium-sized (<19μm)	10.6±1.4	10.5±1.5	10.5±1.4
GluR4	Large (≥19μm)	24.5±2.4	25.8±3.4	26.1±2.9
GluR4	Medium-sized (<19μm)	13.6±1.8	13.8±1.6	13.7±1.8

N=3

Abbreviations: CALB, calbindin; PARV, parvalbumin; ChAT, choline acetyltransferase; SS, somatostatin; CALR, calretinin.

Table 2
Immunolabeled Neuron Types as Percent of all Striatal Neurons in Monkey

Frequency of the different types of immunolabeled perikarya in the rhesus monkey striatum. The perikarya immunolabeled for neuronal markers (ChAT, PARV, CALR, SS, CALB) and GluR1, GluR2, GluR2/3, and GluR4 are expressed as a percentage of NeuN labeled perikarya in adjacent sections of that region (caudate and putamen, respectively). Some AMPA units and neuron types are divided into subcategories based on their staining intensity and/or perikaryal size (large ≥19μm; medium-sized <19μm). Frequencies are expressed as mean ± SD.

Marker	Labeled Neuron Categories	Caudate	Putamen	Combined
CALB	All	95.1±18.1% (matrix)	82.8±20.3% (striosome+matrix)	88.9±19.3%
CHAT	All	1.1±0.2%	0.9±0.2%	1.0±0.2%
PARV	All	1.0±0.2%	2.4±0.3%	1.7±0.8%
CALR	Large (≥19μm)	0.3±0.1%	0.3±0.1%	0.3±0.1%
CALR	Medium-sized (<19μm)	8.8±2.0%	3.9±0.7%	6.3±2.7%
SS	Medium-sized (<19μm)	1.9±0.5%	1.2±0.4%	1.5±0.5%
GluR1	Large (≥19μm) (moderately labeled)	1.6±0.8%	1.0±0.3%	1.3±0.6%
GluR1	Medium-sized (<19μm) (moderately labeled)	45.8±12.3%	47.1±11.9%	46.4±9.8%
GluR1	Large (≥19μm) (intensely labeled)	0.2±0.1%	0.2±0.1%	0.2±0.1%
GluR1	Medium-sized (<19μm) (intensely labeled)	18.2±4.2%	15.1±1.7%	16.6±3.3%
GluR2	Large (≥19μm)	0.6±0.3%	0.7±0.2%	0.6±0.2%
GluR2	Medium-sized (<19μm)	76.9±12.6%	79.5±3.9%	78.2±8.4%
GluR2/3	Large (≥19μm)	0.9±0.8%	1.4±0.5%	1.1±0.6%
GluR2/3	Medium-sized (<19μm)	76.0±9.3%	71.7±8.1%	74.0±8.2%
GluR4	Large (≥19μm)	0.6±0.1%	0.5±0.2%	0.5±0.1%
GluR4	Medium-sized (<19μm)	2.0±0.1%	1.9±0.1%	1.9±0.1%

N=3

Abbreviations: CALB, calbindin; PARV, parvalbumin; ChAT, choline acetyltransferase; SS, somatostatin; CALR, calretinin.

Table 3
Neuron Types as Inferred Percent of all Striatal Neurons in Monkey

Inferred frequencies of the major striatal neuron types studied here. See text for explanation of how these estimates were derived.

Marker	Labeled Neuron Categories	Caudate	Putamen
CALB	Projection Neurons	94%	94%
ChAT	Interneuron	1.1%	0.9%
PARV	Interneuron	1.0%	2.4%
CALR	Subset of cholinergic interneuron	0.3%	0.3%
CALR	Medium-sized interneuron	2.0%	1.5%
CALR	Subset of projection neurons	6.8%	2.4%
SS	Interneuron	1.9%	1.2%

Abbreviations: CALB, calbindin; PARV, parvalbumin; ChAT, choline acetyltransferase; SS, somatostatin; CALR, calretinin.

Table 4

Inferred Percent of Striatal Neuron Types Possessing Immunodetectible Levels of Specific AMPA Subunits in Monkey

Inferred frequencies of the GluR1-4 localization on three of the major striatal neuron types studied here. See text for explanation of how these estimates were derived.

Neuron Type	GluR1 moderate	GluR1 intense	GluR2	GluR3	GluR4
Projection Neuron	45%	14%	75%	?	?
Cholinergic Interneuron	95%	5%	50%	50%	40%
PARV Interneuron	0	100%	>25%	?	80%

Table 5
Information on the Antibodies Used in This Study

Information on the primary antibodies used in the present study, with their dilutions, animal host, supplier, and key references indicating antibody specificity.

Antibody	Dilution	Animal source	Company	References
GluR1	1–3μg/ml	rabbit	Chemicon International Inc., Temecula, CA	Patralia and Wenthold, 1992
GluR2/3	1–3μg/ml	rabbit	Chemicon International Inc., Temecula, CA	Wenthold et al., 1992
GluR2	1–3μg/ml	mouse	Chemicon International Inc., Temecula, CA	Vissavajjhala et al., 1996
GluR4	1–3μg/ml	rabbit	Chemicon International Inc., Temecula, CA	Wenthold et al., 1992
CALB	1:500	mouse	Sigma-Aldrich, St. Louis, MO	Celio et al., 1990
ChAT	1:100	goat	Chemicon International Inc., Temecula, CA	Shiromani et al., 1987
SS	1:100	mouse	Drs. J.C. Brown & S.R. Vincent, Vancouver, BC, Canada	Vincent and Johansson, 1983
CALR	1:1000	mouse	Swant, Bellinzona, Switzerland	Zimmermann and Schwaller, 2002
NeuN	1:1000	mouse	Chemicon International Inc., Temecula, CA	Mullen et al, 1992

CALB, calbindin; PARV, parvalbumin; ChAT, choline acetyltransferase; SS, somatostatin; CALR, calretinin.